Formation of emerging DBPs from the chlorination and chloramination of seawater algal organic matter and related model compounds

Thesis by

Maolida Nihemaiti

In Partial Fulfillment of the Requirements

For the Degree of

Master of Science

King Abdullah University of Science and Technology

Thuwal, Kingdom of Saudi Arabia

May 2014

EXAMINATION COMMITTEE APPROVALS FORM

The thesis of Maolida Nihemaiti is approved by the examination committee.

Committee Chairperson: Jean-Philippe Croué
Committee Member: TorOve Leiknes
Committee Member: Peiying Hong

ABSTRACT

Formation of emerging DBPs from the chlorination and chloramination of seawater algal organic matter and related model compounds

Maolida Nihemaiti

Limited studies focused on reactions occurring during disinfection and oxidation processes of seawater. The aim of this work was to investigate disinfection by-products (DBPs) formation from the chlorination and chloramination of seawater algal organic matter and related model compounds. Simulated algal blooms directly growing in Red Sea, red tide samples collected during an algal bloom event and *Hymenomonas* sp. monoculture were studied as algal organic matter sources. Experiments were conducted in synthetic seawater containing bromide ion. A variety of DBPs was formed from the chlorination and chloramination of algal organic matter. Brominated DBPs (bromoform, DBAA, DBAN and DBAcAm) were the dominant species. Iodinated DBPs (CIAcAm and iodinated THMs) were detected, which are known to be highly toxic compared to their chlorinated or brominated analogues. Algal organic matter was found to incorporate important precursors of nitrogenous DBPs (N-DBPs), which have been reported to be more toxic than regulated THMs and HAAs. Isotopically-labeled monochloramine (^{15}N-NH_2Cl) was used in order to investigate the nitrogen source in N-DBPs. High formation of N-DBPs was found from *Hymenomonas* sp. sample in exponential growth phase, which was enriched in nitrogen-containing organic compounds. High inorganic nitrogen incorporation was found from the algal samples enriched in humic-like compounds. HAcAms formation was studied from chlorination and chloramination of amino acids. Asparagine, aspartic acid and other amino acids with an aromatic structure were found to

be important precursors of HAcAms and DCAN. Factors affecting HAcAms formation (Cl_2/ amino acid molar ratio and pH) were evaluated. Studies on the formation kinetics of DCAcAm and DCAN from asparagine suggested a rapid formation of DCAcAm from organic nitrogen (amide group) and a slower incorporation of inorganic nitrogen coming from monochloramine to form DCAN. High amounts of DCAN and DCAcAm were detected from the chloramination of aromatic compounds (i.e., phenol and resorcinol) indicating that N-DBPs can also be formed from organic compounds without any organic nitrogen through the incorporation of inorganic nitrogen from monochloramine. Moreover, results from *Hymenomonas* sp., aromatic amino acids, and phenolic compounds suggested that aromatic compounds are highly reactive with monochloramine and a major fraction of DBP precursors.

ACKNOWLEDGMENTS

Frist and foremost, I would like to express my very great appreciation to my advisor, Prof. Jean-Philippe Croué, for his support, motivation and immense knowledge. He continually and persuasively conveyed a spirit of adventure and great passion in regard to scientific research. Without his supervision and constant help, this research work would not have been possible.

I would like to offer my special thanks to Dr. Julien Le Roux, for his patient guidance and assistance in the past 15 months of research and study. He introduced me into the topic and has been involved in every single step of my thesis work. I am very grateful for his valuable and constructive suggestions throughout the research project. His willingness to give his time so generously has been very much appreciated.

Thanks are due to Prof. David A. Reckhow at University of Massachusetts Amherst, for his helpful instructions and great support. I also want to thank Yun Yu and Sherrie for their kind assistance during my stay in Prof. Reckhow's lab.

My appreciation also goes to Dr. Tony Merle, Dr. Muhammed T. Khan, and Laure Dramas from Prof. Croué's research group, for providing me with algae and water samples.

My special thanks are extended to my thesis committee members, Prof. TorOve Leiknes and Prof. Peiying Hong.

I wish to thank my friends, Murat, Liu Han, Yang Yanchao, Dr. Wang Yuru, and Lv Dongwei, for their friendships and great support.

I would also like to extend my gratitude to all of my colleagues in Prof. Croué's research group and Water Reuse and Desalination Center at KAUST.

Last but not least, I would like to express my deep gratitude to my parents, for their unconditional love and support. My heartfelt gratitude is extended to my lovely sisters and brother for their continuous encouragements.

TABLE OF CONTENTS

LIST OF ABBREVIATIONS

AOM	Algal organic matter
EOM	Extracellular organic matter
IOM	Intracellular organic matter
DBPs	Disinfection by-products
N-DBPs	Nitrogenous disinfection by-products
C-DBPs	Carbonaceous disinfection by-products
NOM	Natural organic matter
TOC	Total organic carbon
TON	Total organic nitrogen
FEEM	Fluorescence excitation-emission matrix
SUVA	Specific ultraviolet absorbance
THMs	Trihalomethanes
HAAs	Haloacetic acids
HANs	Haloacetonitriles
HAcAms	Haloacetamides
HNMs	Halonitromethanes
NDMA	N-nitrosodimethylamine
DCAA	Dichloroacetic acid
DCAN	Dichloroacetonitrile
TCAN	Trichloroacetonitrile
TCNM	Trichloronitromethane
DCAcAm	Dichloroacetamide

LIST OF ILLUSTRATIONS

LIST OF TABLES

Introduction

Prechlorination is used in seawater desalination processes to control biofouling in both thermal plants and membrane plants. Important amounts of disinfectant can be required to maintain a residual during algal bloom events.

Algal blooms cause challenges in water treatment processes, because algae and algal metabolites affect the water quality by releasing taste, odors and toxins (Nguyen et al. 2005, Plummer and Edzwald 2002) and algal blooms are a major cause of membrane fouling in desalination plants (Her et al. 2004). Additionally, algal organic matter (AOM) is an important precursor of disinfection by-products (DBPs) (Fang et al. 2010a, Fang et al. 2010b, Nguyen et al. 2005).

AOM is enriched in organic nitrogen, which is potentially precursor of nitrogenous DBPs (N-DBPs). N-DBPs generally form in much smaller amounts than regulated DBPs, such as trihalomethanes (THMs) and haloacetic acids (HAAs), but have been a growing concern because of their greater health risk (Muellner et al. 2007, Plewa et al. 2004). *In vitro* mamallian cell tests demonstrated that haloacetonitriles (HANs), halonitromethanes (HNMs) and haloacetamides (HAcAms) are more cytotoxic and genotoxic (up to 2 orders of magnitude) than non-nitrogenous THMs and HAAs (Plewa et al. 2008).

As an alternative disinfectant, monochloramine (NH_2Cl) is often used in distribution networks and cooling systems to get a more stable disinfectant residual. However, NH_2Cl can be an additional source of nitrogen and leads to the formation of N-DBPs (e.g., N-nitrosodimethylamine (NDMA)).

Moreover, bromide and iodide ions exist in seawater in high levels. The concentrations of bromide and iodide in seawater are 60 mg/L (Flury and Papritz 1993) and 45-65 µg/L (Bichsel and Von Gunten 1999, Fuge and Johnson 1986), respectively. Presence of bromide and iodide ions in seawater favors the formation of brominated and iodinated byproducts that are often more toxic than their chlorinated analogues (Richardson et al. 2008, Richardson et al. 2007).

Some previous studies focused on the characterization of AOM and DBPs formation potential from the chlorination of fresh water (Fang et al. 2010a, Fang et al. 2010b, Huang et al. 2009, Nguyen et al. 2005). However, limited studies focused on the DBPs formation from the disinfection of seawater in the presence of AOM, especially the formation of emerging classes of DBPs (i.e., N-DBPs, brominated and iodinated DBPs). Moreover, limited information is available about the role of monochloramine in N-DBPs formation during the chloramination of AOM in seawater matrix.

HAcAms represent an emerging class of N-DBPs. Plewa et al. (2008) found that the HAcAms are highly toxic. They are 99x, 2x and 1.4x more cytotoxic than HAAs, HANs and HNMs, respectively. Moreover, they are 19x and 2.2x more genoctoxic than HAAs and HNMs, respectively.

Literature about the formation mechanism of HAcAms and their precursors in natural organic matter (NOM), wastewater, algal organic matter or seawater organic matter is limited. The HAcAms formation potential of some amino acids (Chu et al. 2010b, Huang et al. 2012) humic acid, wastewater effluent and algal extracellular polymeric substances (EPS) (Huang et al. 2012) and bacteria culture (Huang et al. 2013) were reported but no

studies were focused on seawater algal organic matter. Two reaction pathways have been proposed for the formation of HAcAms during water disinfection. The first one is the decarboxylation pathway, producing HANs that are then hydrolyzed into HAcAms. In this case, the nitrogen atom of HAcAms is coming from the precursor compound (i.e., amino acids, organic nitrogen) (Huang et al. 2012). The second reaction pathway is the aldehyde pathway, where NH_2Cl reacts with aldehydes to produce HANs and HAcAms (Kimura et al. 2013). In this case, the nitrogen atom of NH_2Cl is incorporated into HAcAms.

This study investigates the DBPs formation potential from the chlorination and chloramination of different AOM sources (i.e., simulated algal bloom grown in Red Sea, real red tide samples collected during an algal bloom event and *Hymenomonas* sp. monocultures in different growth phases). Synthetic seawater with bromide ion (70.3 mg/L) was used in order to get close to the real situation during seawater disinfection process. Isotopically-labeled monochloramine (^{15}N-NH_2Cl) was applied for exploration of nitrogen source in N-DBPs.

Model precursors (i.e., amino acids and phenolic compounds) were also studied to evaluate the factors (i.e., molecular structure, Cl_2 to amino acid molar ratio, pH and reaction time) influencing the formation of N-DBPs, especially the HAcAms.

1. Literature review

1.1 Algal Organic Matter (AOM)

AOM includes extracellular organic matter (EOM) and intracellular organic matter (IOM). EOM is released via metabolic excretion, while IOM is a result of cell lysis. AOM has different characteristics from NOM. Understanding the properties of AOM is essential to determine the precursors of algal-associated DBPs.

AOM comprises proteins, amino sugars, aliphatic amines, peptides, carbohydrates, nucleic acids, lipids, chlorophyll and other organic matter. Her et al. (2004) reported that blue-green algae incorporates 68% protein, 22% carbohydrate, 5% lipids and 3% chlorophyll. Moreover, the composition of amino acids, carbohydrate and lipid is affected by the growth phase (Brown et al. 1993).

The C:N ratio of AOM is much lower than NOM. Fang et al. (2010b) found that the total organic carbon (TOC)/ total organic nitrogen (TON) ratio of *Microcystis aeruginosa* (blue-green algae) followed this order: NOM>>EOM>IOM≈algal cells. Much lower C:N ratio indicates high organic nitrogen (org-N).

Figure1 shows the Fluorescence Excitation-Emission Matrix (FEEM) for the EOM, IOM, and algal cell of *Microcystis aeruginosa* and Suwannee River NOM (Fang et al. 2010b). EOM, IOM and algal cell exert high fluorescence signal in regions II and IV, which is attributed to protein-like organic matter or org-N rich compounds, while NOM is rich in humic-acid like and fulvic-acid like matter with high signal in regions III and V (Figure 2) (Chen et al. 2003).

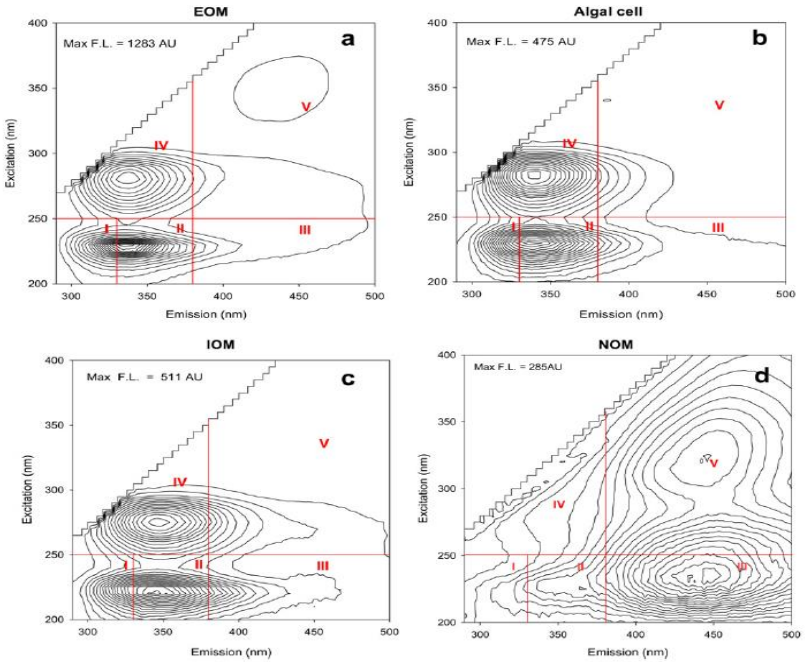

Figure 1. Fluorescence EEMs of EOM, IOM, algal cell and NOM (Fang et al. 2010b)

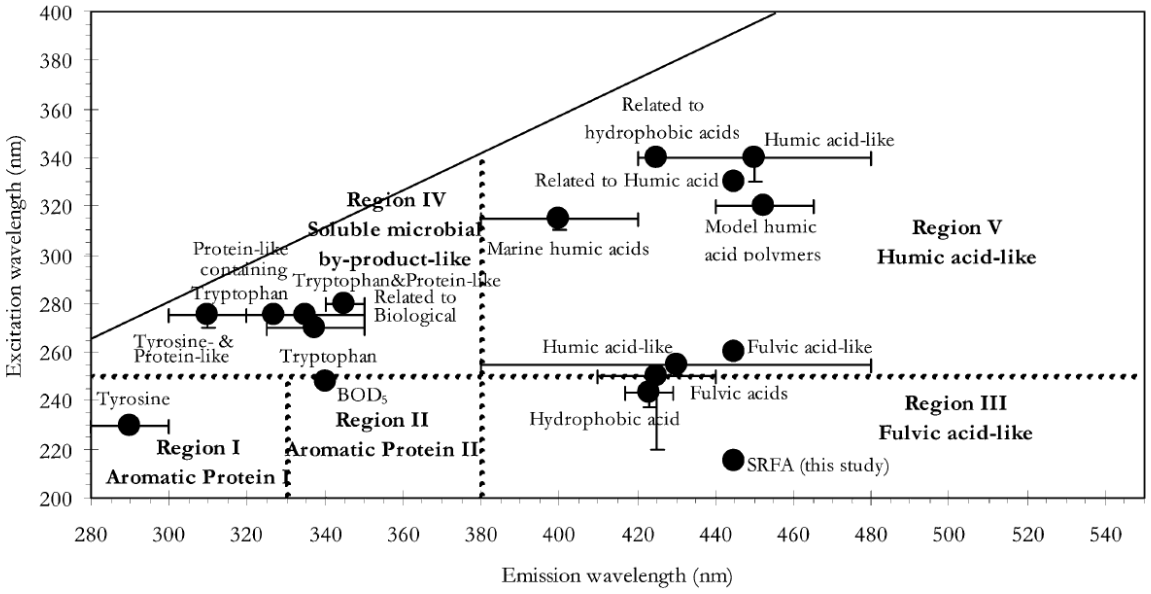

Figure 2. Fluorescence EEM Regions (Chen et al. 2003)

AOM is enriched in hydrophilic substances showing low Specific Ultraviolet Absorbance (SUVA) (Henderson et al. 2008, Her et al. 2004, Li et al. 2012), which indicates the low aromatic carbon content.

Nguyen et al. (2005) found that more than 60% of AOM from *Scenedesmus* (green algae) was biodegradable organic carbon and most of it was probably amino sugars, amino acids and carbohydrates. Rostad et al. (1997) hypothesized that colloidal NOM, mainly amino sugars, was biodegradable and transformed into humic materials with higher C/N ratio.

EOM can be released from algae cells during the growth phase and among them, polysaccharides can comprise 80-90% of the total extracellular release (Myklestad 1995). The org-N composition of EOM and IOM from *Microcystis aeruginosa* (blue-green algae) has been characterized in details (Fang et al. 2010b). IOM had a higher concentration of TON than EOM and the measured free amino acids (e.g., arginine, lysine) and aliphatic amines (e.g., diethylamine, ethylamine) comprised only 2.5% and 11.3% of TON in EOM and IOM, respectively (Fang et al. 2010b).

1.2 Chemistry of chlorine and chloramines

1.2.1 Chlorine

Chlorine is a powerful oxidant and widely used in water treatment processes as disinfectant due to its low cost and strong ability to inactivate a wide variety of pathogenic microorganism (Connell 1996, Desiderio and Nibbering 2010). It is also commonly applied in power plants cooling water system and seawater desalination plants for bio-fouling control.

Chlorine gas forms hypochlorous acid (HOCl) in water via rapid hydrolysis.

$$Cl_2 + H_2O = HOCl + H^+ + Cl^- \qquad (1)$$

$k_1=3.94 \times 10^{-4}\ M^2$ at 25 ˚C (Connick and Chia 1959)

Chlorine is also in equilibrium with trichloride ion (Cl_3^-):

$$Cl_2 + Cl^- = Cl_3^- \quad (2)$$

k_2= 1.91 x 10^{-1} M at 25 ˚C (Zimmerman and Strong 1957)

Hypochlorous acid is a weak acid and dissociates to hypochlorite ion.

$$HOCl = ClO^- + H^+ \quad (3)$$

k_3= 2.90 x 10^{-8} M = $10^{-7.53}$ at 25 ˚C (Carrell Morris 1966)

Sum of these four species (Cl_2, HOCl, ClO^- and Cl_3^-) is called free chlorine.

Moreover, chlorine can oxidize bromide and iodide ions in water (e.g., seawater). Bromide ion is oxidized to hypobromous acid (HOBr).

$$HOCl + Br^- \rightarrow HOBr + Cl^- \quad (4)$$

k_4= 2.46 x 10^7 $M^{-1}h^{-1}$ (Bousher et al. 1989)

In the presence of iodide, hypoiodous acid can be formed as well, but is rapidly oxidized to iodate ion (IO_3^-) (Equation 6).

$$HOCl + I^- \rightarrow HOI + Cl \quad (5)$$

k_5=4.3 x 10^8 $M^{-1}s^{-1}$ (Nagy et al. 1988)

$$2\ HOCl + HOI \rightarrow IO_3^- + 2\ Cl^- + 3\ H^+ \quad (6)$$

k_6= 8.3 x 10^4 $M^{-2}s^{-1}$ (Bichsel and Von Gunten 1999)

HOBr reacts with NOM faster than HOCl and HOI.

$$HOCl + NOM \rightarrow Products \quad (7)$$

k_7=0.7-5 $M^{-1}s^{-1}$ (Westerhoff et al. 2004)

$$HOBr + NOM \rightarrow Products \quad (8)$$

k_8=15-167 $M^{-1}s^{-1}$ (Westerhoff et al. 2004)

$$HOI + NOM \rightarrow Products \quad (9)$$

k_9=0.1-0.4 $M^{-1}s^{-1}$ (Bichsel and Von Gunten 2000)

1.2.2 Chloramines

Monochloramine (NH_2Cl) is often used as alternative disinfectant to chlorine because of the reduced formation of regulated disinfection by-products (i.e., THMs and HAAs). It is often used in power plants cooling systems and as final disinfection in drinking water treatment plants in several countries (e.g., USA, Australia).

Chloramines are formed through the reaction between aqueous chlorine and ammonia (NH_4^+/NH_3). Monochloramine (NH_2Cl), dichloramine ($NHCl_2$) and nitrogen trichloride (NCl_3) can be specifically formed by adjusting the N:Cl ratio.

$$NH_4^+ + HOCl \rightarrow NH_2Cl + H_3O^+ \quad (10)$$

k_{10}=1.5 x 10^{10} $M^{-1}\cdot h^{-1}$ (Morris and Isaac 1983)

$$NH_2Cl + HOCl \rightarrow NHCl_2 + H_2O \quad (11)$$

k_{11}= 1.0 x 10^6 $M^{-1}\cdot h^{-1}$ at 25 °C (Gray Jr et al. 1978)

$$NHCl_2 + HOCl \rightarrow NCl_3 + H_2O \quad (12)$$

k_{12}= 1.59 x 10^6 $M^{-1}\cdot h^{-1}$ at 25 °C (Hand and Margerum 1983)

The sum of chloramine species (NH_2Cl, $NHCl_2$ and NCl_3) is called combined chlorine. Figure 3 gives the relationship between Cl_2:N ratio and chloramine species. When the Cl_2:N ratio is less than 5 by weight, monochloramine will predominate. Break point reaction occurs when the Cl_2:N ratio increases from 5 to 7.6. At the break point, the residual chlorine concentration is reduced to a minimum. 7.6 is a theoretical value. Free chlorine and trichloride will be formed when the Cl_2:N ratio further increases.

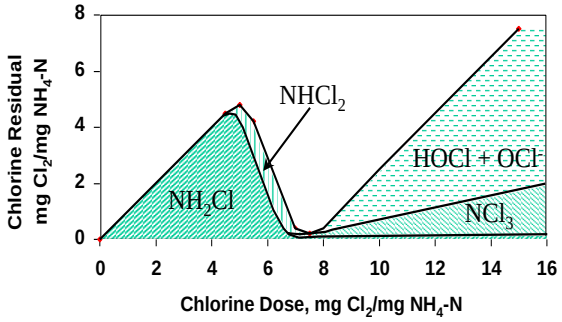

Figure 3. Theoretical Breakpoint Curve (USEPA 1999)

Moreover, pH affects the distribution of chloramines species in water (Figure 4). At pH>7, the major species is monochloramine.

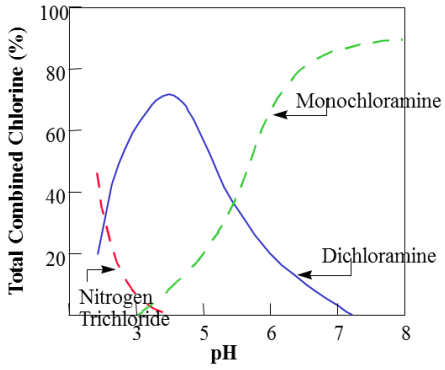

Figure 4. Distribution diagram for chloramines species as a function of pH (USEPA 1999)

Additionally, monochloramine is known to oxidize bromide ion to bromochloramine (NHBrCl) (Equation 13) (Trofe 1980). Bromochloramine is less stable than chloramines. NHBrCl reacts with NH_2Cl (Equation 14) (Vikesland et al. 2001), explaining the catalytic role of bromide in chloramine decomposition.

$$NH_3Cl^+ + Br^- \rightarrow NH_3Br^+ + Cl^- \quad (13)$$

k_{13}= 5.0 x 10^4 $M^{-1}\cdot s^{-1}$ at 25 ˚C (Trofe 1980)

$$NHBrCl + NH_2Cl \rightarrow N_2 + Br^- + 2Cl^- + 3H^+ \quad (14)$$

(Vikesland et al. 2001)

1.3 Disinfection by-products (DBPs)

1.3.1 DBPs occurrence and regulations

During water treatment processes, disinfectants (chlorine, ozone, chlorine dioxide, or chloramines) can react with naturally occurring organic matter, anthropogenic contaminants, bromide, and iodide ions to produce DBPs (Richardson et al. 2007). Chloroform and other THMs were the first DBPs reported in 1970s in chlorinated drinking water (Rook 1975). During the last 30 years, more than 600 DBPs have been reported and raised public concern due to their potential genotoxicity and carcinogenicity. However, only a small number of them were quantified and their health-effects investigated (Richardson et al. 2007). The World Health Organization (WHO) published guidelines on part of these DBPs to control their amount in drinking water (Table1). A large variety of DBPs are still unregulated (e.g., iodinated THMs).

Table 1. World Health Organization (WHO) DBP guidelines (Richardson et al. 2007)

DBP	Guideline value (mg/L)
Chloroform	0.2
Bromodichloromethane	0.06
Chlorodibromomethane	0.1
Bromoform	0.1
Dichloroacetic acid	0.05[a]
Trichloroacetic acid	0.2
Bromate	0.01[a]
Chlorite	0.7[a]
Chloral hydrate (trichloroacetaldehyde)	0.01[a]
Dichloroacetonitrile	0.02[a]
Dibromoacetonitrile	0.07
Cyanogen chloride	0.07
2,4,6-Trichlorophenol	0.2
Formaldehyde	0.9

[a] Provisional guideline value

1.3.2 DBPs formation from AOM

A few studies demonstrated the importance of AOM as a precursor of DBPs. Based on the comparison of two blue-green algae, Huang et al. (2009) found that yields of THMs and HAAs formation increased as the dissolved organic carbon (DOC) increased during the growth phase. Other studies also reported that the chloroform concentration increased with time (Nguyen et al. 2005). Under the same experimental conditions, comparable amounts of dichloroacetic acid (DCAA) were detected from the chlorination of AOM than Suwannee River NOM, but higher amounts of nitrogenous DBPs (N-DBPs) were formed from AOM than from NOM (Fang et al. 2010a). Preozonation was found to

significantly increase the carbonaceous DBPs (C-DBPs) and N-DBPs concentration by releasing IOM through cell lysis (Xie et al. 2013).

Additionally, the influence of reaction time, chlorine dosage, pH and temperature on AOM-derived DBPs formation was evaluated (Fang et al. 2010a). The C-DBPs (i.e., THMs, HAAs) concentration increased rapidly during the first 3 days and then slowed down, while for N-DBPs, (i.e., dichloroacetonitrile (DCAN), trichloroacetonitrile (TCAN) and trichloronitromethane (TCNM)), the concentration decreased after 3 days. Most of DBPs' formation increased with chlorine dosage. However, DCAN decreased rapidly when the chlorine dosage was more than 10.2 mg/L as Cl_2. The yields of chloroform and HAAs increased when the pH was raised from 4 to 7, but the maximum amount of DCAN was detected at pH 6. All of these DBPs (i.e., THMs, HAAs, DCAN, TCAN, TCNM) increased when the temperature was changed from 10 ^{o}C to 25 ^{o}C. However, the influence of those parameters (i.e., contact time, pH, temperature, chlorine dosage and Cl:N ratio) on the formation of N-DBPs, especially HAcAms, is still unknown.

The DBPs formation potentials of IOM, EOM and algae cells were compared (Huang et al. 2009, Li et al. 2012). Huang et al. (2009) found that Anabaena flos-aquae and *Microcystis aeruginosa* (two blue-green algae species) algae cells produced more THMs and HAAs than their corresponding EOM. However, Li et al. (2012) reported higher formation potentials of THMs, HAAs and N-DBPs (e.g., NDMA) from *Microcystis aeruginosa* IOM as compared to its EOM. As mentioned earlier, IOM contains higher TON than EOM, including free amino acids and aliphatic amines, which contribute to the significant DBPs formation potential of IOM. This result indicates that it is critical to remove the algae cells and prevent their damage to release IOM in order to decrease the

DBPs formation during the water treatment process. However, the formation potential of other N-DBPs (e.g., HAcAms) from IOM and EOM has not been studied.

The nitrogenous organic fraction of AOM can be the precursor of N-DBPs. However, some studies found that inorganic nitrogen from chloramines also play a significant role in N-DBPs formation. For example, NH_2Cl reacts with dimethylamine to produce NDMA during chloramination (Choi and Valentine 2002). Nitrogen incorporation from NH_2Cl has also been observed in the formation of cyanogen chloride from formaldehyde (Pedersen III et al. 1999). Previous studies used isotopically-labeled monochloramine ($^{15}NH_2Cl$) for the nitrogen origin exploration during the chloramination of nitrogenous organic compounds and natural organic matter (Chuang et al. 2013, Yang et al. 2010). It was reported that during the chloramination of tryptophan and Suwannee River NOM, the percentages of ^{15}N-DCAN in total DCAN were 78% and 92%, respectively, indicating the high amount of nitrogen incorporation from monochloramine (Yang et al. 2010).

1.3.3 Nitrogenous DBPs

Occurrence of N-DBPs in drinking water raised concern because of their high genotoxicity and cytotoxicity compared to regulated DBPs. Important N-DBPs include HANs, HAcAms, Cyanogen halides, HNMs and Nitrosamines (Table2) (Bond et al. 2011).

Wastewater discharge and algal organic matter presence in water source lead to the significant increase in N-DBPs formation (Bond et al. 2012). Wastewater effluents, algal

EPS and free amino acids (i.e., aspartic acid, asparagine) have been reported to produce HANs and HAcAms (Huang et al. 2012).

The use of alternative disinfectant (i.e., chloramines), can also increases the concentration of some N-DBPs (e.g., NDMA) (Choi and Valentine 2002).

Table 2. Classes of nitrogenous disinfection by-products (N-DBPs) (Bond et al. 2011)

Group/formula	Structure	Important species	Structure
Haloacetonitriles (HANs) R_3CCN	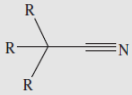	Dichloroacetonitrile (DCAN) (right), bromochloroacetonitrile (BCAN), dibromoacetonitrile (DBAN), trichloroacetonitrile (TCAN) and tribromoacetonitrile (TBAN)	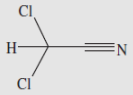
Haloacetamides (HAcAms) R_3CCONH_2	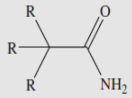	Dichloroacetamide (DCAcAm) (right), dibromoacetamide (DBAcAm), trichloroacetamide (TCAcAm)	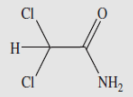
Cyanogen halides (CNX) RCN	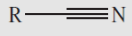	Cyanogen chloride (CNCl) (right), cyanogen bromide (CNBr)	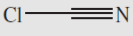
Halonitromethanes (HNMs) R_3CNO_2	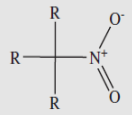	Trichloronitromethane (chloropicrin) (right), tribromonitromethane (bromopicrin), bromodichloronitromethane, dibromochloronitromethane	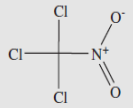
Nitrosamines R_2NNO	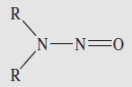	N-nitrosodimethylamine (NDMA) (right), N-nitrosopyrrolidine (NPYR), N-nitrosomorpholine (NMOR), N-nitrosodiethylamine (NDEA)	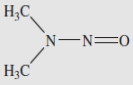

R is typically Cl, Br, I, H or an alkyl group, though it can also be a larger aliphatic or aromatic group.

1.3.4 Haloacetamides, an Emerging Class of Nitrogenous DBPs

HAcAms represent an emerging class of N-DBPs. Plewa et al. (2008) found that the HAcAms are highly toxic. They are 99x, 2x and 1.4x more cytotoxic than HAAs, HANs and HNMs, respectively. Moreover, they are 19x and 2.2x more genotoxic than HAAs and HNMs, respectively. In general, the toxicity was determined by the type of halogen and followed this order: I>Br>>Cl.

It is known that HAcAms are intermediate products of HANs hydrolysis (Glezer et al. 1999, Reckhow et al. 2001). Recently, Huang et al. (2012) reported that HAcAms can be formed independently. For example, the amide group in asparagine can lead to the production of dichloroacetamide (DcAcAm) without the formation of DCAN as an intermediate.

1.3.4.1 Reaction pathways of haloacetamides formation

There are limited studies regarding the nature of the precursors and reaction mechanism of HAcAms.

HANs degrade to form HAcAms through base catalyzed hydrolysis, then HAcAms are further converted to HAAs (Figure 5) (Reckhow et al. 2001). The degradation of HANs is enhanced at alkaline pH. This process can also be catalyzed by hypochlorite ion and hypochlorous acid. However, HAcAms degradation rate at different pHs and in the presence of chlorine/chloramines is still unknown.

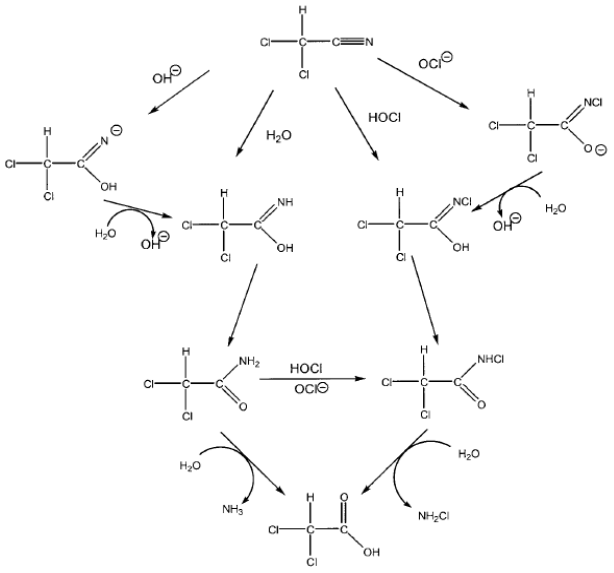

Figure 5. DCAN hydrolysis (Reckhow et al. 2001)

Two different pathways have been proposed for HANs formation. The first one is the decarboxylation pathway during the chlorination of free amino acids. Free chlorine reacts rapidly with α-amine group of free amino acids to form aldehydes or nitriles, then nitriles are further hydrolyzed to form HAcAms (Figure 6). Similar reaction happens during chloramination, but needs higher exposure. During chloramination, [Cl] can be transferred from monochloramine to α-amine group with a slower rate than chlorine (Lee and Westerhoff 2009, Shah and Mitch 2012, Yang et al. 2010).

The formation of dichlorinated α-amino group is favored when free chlorine/chloramine to amino acids ratio increases (Yang et al. 2010).

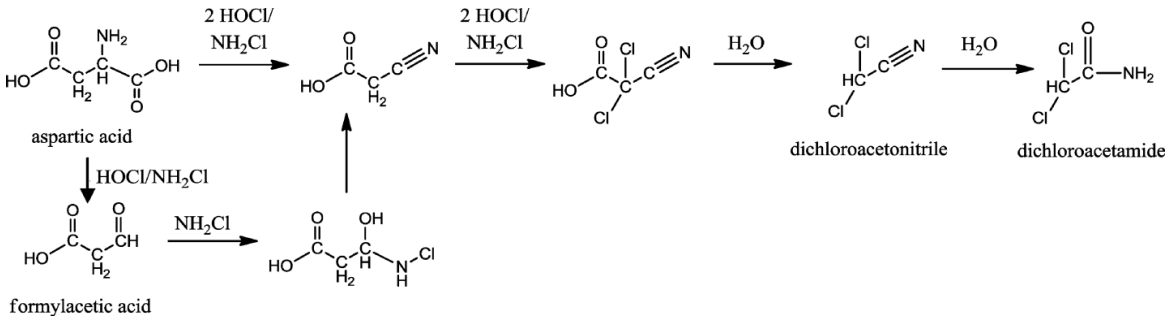

Figure 6. Chlorination and Chloramination reaction mechanisms of Aspartic acid (Huang et al. 2012)

The second pathway of HANs formation is the aldehyde pathway, where monochloramine reacts with aldehydes to produce nitriles. Pedersen III et al. (1999) reported the formation of cyanogen chloride (CNCl) from the reaction of monochloramine with formaldehyde (Figure 7).

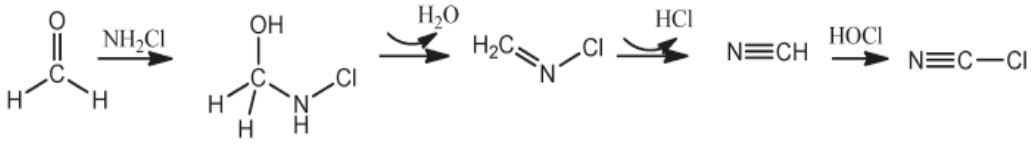

Figure 7. Chloramination of formaldehyde (Shah and Mitch 2012)

Limited information is available on the formation of HAcAms from other aldehydes (especially haloacetaldehydes). Recently, Kimura et al. (2013) reported that chloroacetaldehyde reacted with monochloramine to produce chloroacetonitrile and N,2-dichloroacetamide (Figure 8).

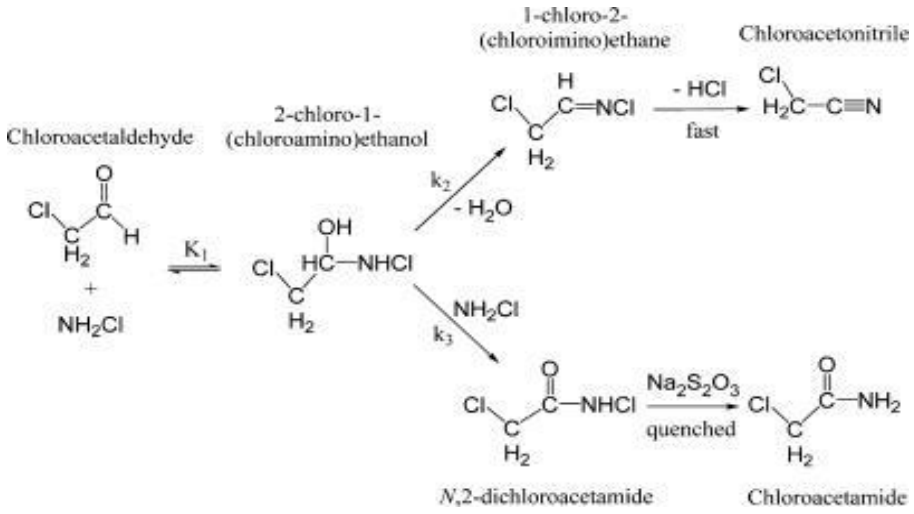

Figure 8. Chloramination of chloroacetaldehyde (Kimura et al. 2013)

During chlorination and chloramination, both decarboxylation and aldehyde pathways can take place. In the decarboxylation pathway, the nitrogen atom of N-DBPs is coming from the nitrogenous organic precursor (e.g., aspartic acid), while in the aldehyde pathway, nitrogen is incorporated from NH_2Cl. Hence, the use of isotopically-labeled monochloramine ($^{15}NH_2Cl$) may be helpful to distinguish the decarboxylation pathway from the aldehyde pathway. Huang et al. (2012) applied $^{15}NH_2Cl$ to the free amino acid asparagine as model precursor and found that the ^{15}N incorporated percentage in

DCAcAm was less than 3%. This result suggested that most of the nitrogen in DCAcAm originated from asparagine and not through the aldehyde pathway.

1.3.4.2 Precursors of haloacetamides

The HAcAm formation potential of different natural waters and model compounds (i.e., amino acids) were examined (Chu et al. 2012, Chu et al. 2013, Chu et al. 2010a, Chu et al. 2010b).

Linear relation (R^2=0.96) between dissolved organic nitrogen (DON)/DOC ratio and HAcAms concentration during chlorination has been reported. Therefore, N-rich organic matters were considered as important precursors. However, for chloramination reaction, this relation was not significant (R^2=0.65) (Chu et al. 2013), which indicated the incorporation of inorganic N from chloramine. Humic or fulvic acid-like substances produced little or no HAcAms. Contrarily, protein-like organic matters formed more (Chu et al. 2010b). During chlorination, asparagine, aspartic acid, glutamine, histidine, phenylalanine, tryptophan, tyrosine produced high concentrations of HAcAms (Chu et al. 2010b). Among them the aspartic acid showed the highest DCAcAm yield.

However, free amino acids are only 6% of the total amino acids found in wastewater and algal impacted raw drinking water supplies (Dotson and Westerhoff 2009). Therefore, protein-derived DBPs studies should focus on combined amino acids (Shah and Mitch 2012). Recently, wastewater effluents, algal EOM and humic substances were found to form DcAcAm during chlorination and chloramination (Huang et al. 2012). These results suggested that the property of DON rather than its amount should be considered as more significant upon N-DBPs formation (Chu et al. 2010b).

1.3.5 Factors influencing the DBPs formation

(Mainly focus on N-DBPs formation)

1.3.5.1 Influence of Cl/N ratio

The formation of DCAcAm during the chloramination of tyrosine increased with the increasing Cl_2/tyrosine molar ratio from 5 to 15, then decreased slightly when this ratio became 25 (Chu et al. 2012).

During the chlorination of aspartic acid, DCAN and DCAA yields reached a maximum of 0.653% and 0.475% at Cl/N = 20.0, respectively. However, a maximum DCAcAm yield of 0.093% was obtained at Cl/N = 1.0 and decreased with the increasing Cl/N (Chu et al. 2010a). This result can be explained by chlorine catalyzed hydrolysis of HAcAms to HAAs (Reckhow et al. 2001).

1.3.5.2 Influence of oxidant exposure

Huang et al. (2012) reported that fast formation of DCAN and DcAcAm happened during chlorination of wastewater effluent , while for chloramination, higher oxidant exposure (i.e., high CT value) was needed.

1.3.5.3 Influence of pH

pH can affect the distribution of disinfectant species in water. For example, OCl^- concentration is higher than HOCl in alkaline condition. NCl_3 formation is favored in acidic conditions (pH<3), while NH_2Cl is the dominant chloramine specie at pH>7 (Figure 4).

pH was found to impact the hydrolysis rate of DBPs. Reckhow et al. (2001) reported that DCAN hydrolysis increased with increasing pH. However, DCAcAm formation from

aspartic acid (50 µmol/L) was negligible at pH 5, was 0.2% molar yield at pH 7 and 0.49 % at pH 9 (Chu et al. 2010a).

1.3.5.4 Influence of bromide and iodide

The presence of bromide and iodide ions in water affects the oxidant species distribution during the disinfection process. As mentioned earlier, both bromide and iodide ions can be oxidized by chlorine and chloramines, and then react with natural organic matter to form brominated and iodinated DBPs. Most brominated and iodinated DBPs were found to be more toxic than their chlorinated homologues (Plewa et al. 2002).

Bromine species ($HOBr/BrO^-$) have been reported as more reactive than equivalent chlorine species (Symons et al. 1993). It was concluded that compared to HOCl, HOBr is a more efficient substitution agent but less efficient oxidant (Hua et al. 2006). Bromine substitution with NOM is faster than chlorine substitution by 1 order of magnitude (Hua et al. 2006, Westerhoff et al. 2004).

Earlier studies demonstrated that with increasing bromide concentration, the THM formation is shifted to more brominated species (Luong et al. 1982). Similar to the THM formation, the increasing concentration of bromide shifts the HAA species to more brominated species, however, the distribution of HAA species among mono-, di- and trihalogenated forms is not influenced by the bromide concentration (Cowman and Singer 1996). During the chlorination of raw waters collected from the drinking water treatment plants, Hua et al. (2006) reported that the increasing bromide concentration doesn't change the TOX concentration, while the increasing iodide concentration leads to the decrease in TOX formation. This indicates the chlorine consumption by the oxidation of

iodide to iodate. The effect of chlorine dose on the iodinated THM (I-THM) and iodate formation was also studied. During the chlorination of raw water spiked with iodide at 2µmol/L, with increasing chlorine dose from 0.5 mg/L to 3 mg/L, the iodate concentration increased, but the I-THM formation exhibited an increasing phase followed by a decreasing phase. This suggests the Cl_2/I ratio is critical in I-THM formation (Hua et al. 2006). Bichsel and Von Gunten (2000) reported that during the oxidation of iodine-containing water, ozone oxidized more than 90% of iodide ions to iodate and there was no I-THM formation. However, during the chlorination, both I-THM and iodate existed, while in chloramination, I-THMs (especially CHI_3) were the major products.

Limited literature is available about the impact of bromide and iodide ions on N-DBPs formation. Heller-Grossman et al. (1999) found that during the chlorination of bromide-rich lake water, increasing the chlorine dose increased the HANs concentration, but decreased cyanogen bromide (CNBr) amount. In contrast to this, Yang et al. (2007) reported that during the chloramination of Suwannee River NOM, with increasing concentration of bromide, the CNX concentration increased, but the HANs decreased.

In seawater, the concentrations of iodine and bromide are 45-65 µg/L (Bichsel and Von Gunten 1999, Fuge and Johnson 1986) and 60mg/L (Flury and Papritz 1993), respectively. Thus the influence of bromide and iodide ions during the chlorination/chloramination of seawater can’t be ignored.

2. Materials and methods

2.1 Materials

Deionized water (18.2 MΩ.cm, TOC<50ppb, Milli-Q, Millipore) was used for all experiments. Buffer solution at pH 7 was prepared using potassium phosphate monobasic (0.0048 M) and sodium phosphate dibasic (0.0052M). Buffer solution at pH 5.5 was prepared using acetic acid (0.0014M) and sodium acetate (0.0085M). Buffer solution at pH 9 was prepared by sodium carbonate (0.0006 M) and sodium bicarbonate (0.0094 M). pH of solutions were adjusted as needed using sodium hydroxide or sulfuric acid (0.1 N, Fisher Scientific).

Sodium hypochlorite (NaOCl, 5.65-6%, Fisher Scientific) and ammonium chloride (Acros Organics, 99.6%) were used as chlorination reagents. ^{15}N-labeled ammonium chloride was purchased from Sigma-Aldrich. Sodium thiosulfate (Fisher Scientific) was used to quench residual oxidant. Amino acids (L-asparagine ≥99.0%, L-aspartic acid ≥99.5%, L-histidine≥99.0%, L-lysine ≥99.0%, L-phenylalanine ≥98%, L-proline ≥99.0%, L-tyrosine ≥98% and L-tryptophan ≥98%), 1,4-Benzoquinone, Phenol and Resorcinol (≥99%) were obtained from Sigma-Aldrich (Table 1).

A mixed standard containing haloacetonitriles (HANs), trichloronitromethane (TCNM) and haloketones (HKs) (EPA 551B Halogenated Volatiles Mix), a mixed standard containing 9 HAAs (EPA 552.2 Methyl Ester Calibration Mix) and surrogate standard decafluorobiphenyl (99%) were supplied from Supelco (Sigma-Aldrich). Chloro-, bromo-dichloro- and trichloroacetamide were obtained from Sigma-Aldrich. Other haloacetamides (HAcAms) were purchased from Cansyn Chem. Corp. Fisher Scientific

Methyl tert-butyl ether (MTBE) and ethyl acetate (> 99%) were used without further purification.

Table 3. Molecular structures of investigated organic compounds

L-asparagine	L-aspartic acid	L-histidine
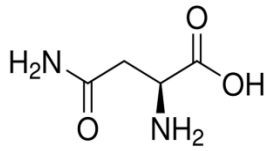	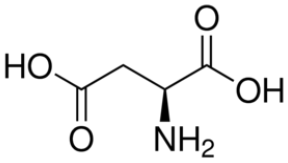	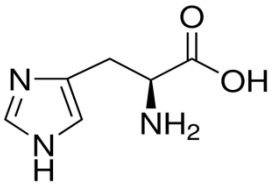
L-phenylalanine	L-proline	L-tyrosine
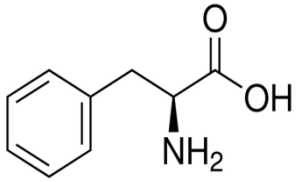	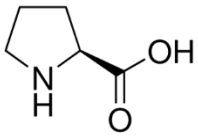	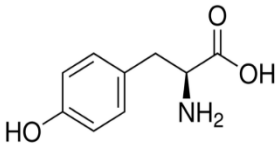
L-tryptophan	Phenol	Resorcinol
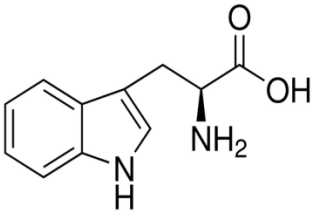	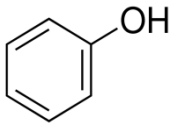	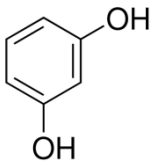

2.2 AOM solutions

10 waterproof mesocosms of 8000 L were built directly in the kaust bay of red sea. There were five different mesocosms samples run in duplicate and grown in different nutrient media for 20 days. In the first sample, NO_3^- (2 µM) and PO_4^{3-} (0.12 µM) were added every day. For the second sample, NO_3^- (16 µM) and PO_4^{3-} (1 µM) were added at the beginning in one shot. Third sample was fed as the first sample, but SiO_3^{2-} (3.75 µM) was also added every day. Fourth sample was fed as second sample, but SiO_3^{2-} (39 µM) was also added in one shot at the beginning. Fifth sample was run as blank. DBPs formation studies were conducted using the first four samples.

A real red tide sample was used as another algal source. This algal bloom occurred along the red sea coast of Saudi Arabia near the city of Yanbu during May 2013. It was identified as a *Trichodesmium* sp. algal bloom. It was in death phase when the experiment was conducted.

Monocultures of *Hymenomonas* sp. in exponential growth phase, stationary growth phase and death phase were used as third algal source. *Hymenomonas* sp. monoculture was cultivated in inorganic culture media within synthetic seawater under a fluorescent lamp with an automated light/dark cycle of 12 h/12 h.

AOM solutions were prepared by filtering the seawater mesocosms, *Trichodesmium* sp. sample and *Hymenomonas* sp. monoculture samples through GF/F filters (Whatman) and diluting the filtrates with synthetic seawater to the desired DOC concentration (1.5 mg/L as C for seawater mesocosms and *Hymenomonas* sp. in exponential phase; 5mg/L as C for *Trichodesmium* sp. and *Hymenomonas* sp. in stationary and death phase). pH was adjusted to pH 8 using NaOH (synthetic seawater pH = 7.6). No additional buffer was used.

Stocks solutions of model organic compounds were prepared by dissolving a pre-determined amount of organic compounds in Milli-Q water based on their solubility.

Preparation and analysis of chlorine and chloramine

Sodium hypochlorite commercial solution was standardized before each experiment by monitoring the absorbance of hypochlorite anion at 292 nm ($\varepsilon = 362\ M^{-1}.cm^{-1}$).

Monochloramine (NH_2Cl) stock solutions (50 mM) were prepared daily by dissolving ammonium chloride (NH_4Cl) in Milli-Q water adjusted to pH = 8.5 with sodium

hydroxide. Sodium hypochlorite (NaOCl) was then added slowly to the rapidly stirred solution, at a Cl:N molar ratio of at least 1:1.2 to avoid breakpoint chlorination resulting from local excess of hypochlorite. Adjusting the pH at 8.5 minimizes the disproportionation of NH_2Cl to dichloramine ($NHCl_2$), since $NHCl_2$ forms at pH < 8 according to equation 1:

$$2NH_2Cl + H^+ = NHCl_2 + NH_4^+ \qquad (1)$$

NH_2Cl and $NHCl_2$ in stock solution were quantified by monitoring absorbances at their respective λ_{max} (λ_{NH2Cl} = 245 nm; λ_{NHCl2} = 295 nm).

Residual oxidant both chlorine and chloramines was analyzed iodometrically (Standards Methods for the Examination of Water and Wastewater, 1995).

2.3 Experimental procedures

All glassware used during the experiments was washed and baked at 500 °C for at least 5 h prior to use. Chlorination/chloramination experiments were carried out using headspace-free 65 mL amber glass bottles at 20 °C in the dark for 72 h. Chlorine or monochloramine was added in excess to AOM solutions (5 mg/L as Cl_2 for seawater mesocosms and *Hymenomonas* sp. in exponential phase; 15 mg/L as Cl_2 for *Trichodesmium* sp. and *Hymenomonas* sp. in stationary and death phase). Chlorine or monochloramine was also added in excess to model organic compound solutions for DBP formation potential experiments (Chlor(am)ine/model compound molar ratio = 5.6 or 14). Each series of experiments included a blank (buffered Milli-Q water). After 72h of reaction time, 5 mL of samples were used for residual chlorine analysis and 3 x 20 mL

were used for DBPs analyses. All samples were quenched with a slight excess of sodium thiosulfate before DBP extraction.

Kinetic of DBPs formation from the chloramination of asparagine at different pH (5.5, 7, 8.8 and 11) was investigated. 50 µmol/L of asparagine was applied. Initial monochloramine concentration was 50 mg/L as Cl_2. In order to avoid DBPs lose, 11 asparagine solutions were prepared in each pH and DBPs were extracted from each solution at different time. DBPs were extracted at 10min, 20 min, 40min, 1h, 2.3h, 4.3h, 6h, 8h, 24h, 48h and 72h.

2.4 Analytical methods

2.4.1 DOC and SUVA analysis

Total Organic Carbon (TOC) and Total Nitrogen (TN) concentrations were measured using a TOC analyzer equipped with a TN total nitrogen detection unit (TOC-VCSH, Shimadzu). UV_{254} absorbance was measured using UV-Vis spectrometer (UV-2550, Shimadzu) and the SUVA was calculated as UV_{254}/DOC and expressed as m^{-1}.L/ mgC.

2.4.2 Fluorescence spectroscopy

Fluorescence Excitation-Emission Matrix (FEEM) was recording using a Aqualog® CDOM Fluorometer (Horiba Scientific, Japan). Excitation spectra and Emission spectra were scanned from 200 nm to 600 nm with 1 nm increment.

2.4.3 DBP analysis

All DBPs analyzed are listed in Table 4.

Four Trihalomethanes (THMs), four haloacetonitriles (HANs), two haloketones (HKs) and chloropicrin were analyzed after liquid-liquid extraction following EPA method 551. 20mL of sample was transferred to a 40mL glass vial containing 4 g of anhydrous sodium chloride. 100 μL of decafluorobiophenyl was added as the internal standard. DBPs were extracted with 3 mL of MTBE. 1μL of solvent was injected (temperature: 200°C) in splitless mode (1mL/min) in an Agilent 7890A gas chromatograph coupled with electron capture detector (GC-ECD). DBPs were separated onto a DB-1701 (30 m x 250 μm x 0.25 μm) column. The column oven was held at 35 ^{o}C for 6 min, ramping to 220 °C at 10 °C/min. The total run time was 24.5 min.

Nine HAAs were extracted and analyzed following the EPA method 552.2, which is based on a liquid-liquid extraction with MTBE in acidic condition followed by derivatization to methyl esters using acidic methanol. 20mL of sample was transferred to a 40mL glass vial containing 4 g of anhydrous sodium chloride. Concentrated sulfuric acid (0.8 mL) was added to adjust the sample pH to acidic condition. After addition of 50 μL of 2-bromopropionic acid as internal standard DBPs were extracted with 4 mL of MTBE. The MTBE layer was transferred to a 10 mL glass vial containing 1 mL of acidic methanol (10 % of sulfuric acid in methanol). The vial was placed in a heating bath at 50 °C. After 2 h, saturated $NaHCO_3$ (4 mL) was added to the vial slowly for neutralization. The vial was shacked for 2 min, and then MTBE layer was further transferred to an autosampler vial. The extract was analyzed using an Agilent 7890A GC system coupled with a 5975C mass spectrometer (GC-MS). The instrument control parameters (i.e., temperature program, column type, injection volume and run time) of GC-MS were the same as those on GC-ECD.

HAcAms were analyzed following the same protocol that was applied for HANs, but MTBE was replaced by ethyl acetate for the liquid-liquid extraction.

Table 4. Description of monitored DBPs

Method of determination	Class of compounds and structures	Abbreviation	Full name
EPA 551	Trihalomethanes (THMs) 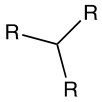	TCM	Trichloromethane (chloroform)
		DCBM	Dichlorobromomethane
		DBCM	Dibromochloromethane
		TBM	Tribromomethane (bromoform)
	Haloacetonitriles (HANs) 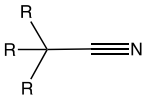	DCAN	Dichloroacetonitrile
		TCAN	Trichloroacetonitrile
		BCAN	Bromochloroacetonitrile
		DBAN	Dibromoacetonitrile
	Haloketones (HKs) 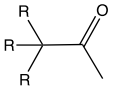	1,1-DCP	1,1-dichloropropanone
		1,1,1-TCP	1,1,1-trichloropropanone
	Halonitromethane 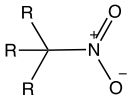	TCNM	Trichloronitromethane
EPA 551 - EA	Haloacetamides (HAcAms)	CAcAm	Chloroacetamide
	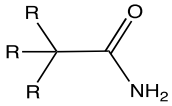	BAcAm	Bromoacetamide
		DCAcAm	Dichloroacetamide
		TCAcAm	Trichloroacetamide
		DBAcAm	Dibromoacetamide
		TBAcAm	Tribromoacetamide

		BCAcAm	Bromochloroacetamide
		CIAcAm	Chloroiodoacetamide
		BIAcAm	Bromoiodoacetamide
		DIAcAm	Diiodoacetamide
EPA 552.2	Haloacetic acids (HAAs) 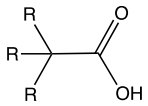	MCAA	Monochloroacetic acid
		MBAA	Monobromoacetic acid
		DCAA	Dichloroacetic acid
		TCAA	Trichloroacetic acid
		BCAA	Bromochloroacetic acid
		DCBAA	Dichlorobromoacetic acid
		DBAA	Dibromoacetic acid
		DBCAA	Dibromochloroacetic acid
		TBAA	Tribromoacetic acid

For experiments involving ^{15}N-NH_2Cl, all solvent extracts were analyzed by GC-MS. Since the ^{15}N-DBPs are not commercially available, the concentration of ^{15}N-DBPs was quantified indirectly using the concentration of unlabeled (i.e, ^{14}N-DBPs). It was reported that the MS response for ^{14}N-DCAN is similar to the MS response for ^{15}N-DCAN, therefore the ^{15}N-DCAN concentration can be determined using the ^{14}N-DCAN standard curve (Huang et al. 2012). The same method was used for other ^{15}N-DBPs analysis. The investigated labeled and unlabeled-DBPs and their related quantification ions are listed table 5.

Table 5. Description of monitored labeled- and unlabeled-DBPs and their quantification ions

Class of compounds	Abbreviation	Quantification ions (m/z)
Haloacetonitriles (HANs)	^{14}N-DCAN	74, 82
	^{15}N-DCAN	75, 82
	^{14}N-TCAN	47, 108, 110
	^{15}N-TCAN	47, 109, 111
	^{14}N-BCAN	74, 76, 155
	^{15}N-BCAN	75, 77, 156
	^{14}N-DBAN	118, 120, 199
	^{15}N-DBAN	119, 121, 200
Haloacetamides (HAcAms)	^{14}N-CAcAm	44, 93, 95
	^{15}N-CAcAm	45, 94, 96
	^{14}N-BAcAm	44, 137, 139
	^{15}N-BAcAm	45, 138, 140
	^{14}N-DCAcAm	44, 83, 127
	^{15}N-DCAcAm	45, 83, 128
	^{14}N-TCAcAm	44, 82, 98
	^{15}N-TCAcAm	45, 82, 98
	^{14}N-DBAcAm	44, 174, 217
	^{15}N-DBAcAm	45, 174, 218
	^{14}N-BCAcAm	44, 171, 173
	^{15}N-BCAcAm	45, 172, 174

3. Results and discussion

3.1 DBPs formation from seawater mesocosms algal bloom AOM

DBPs formation potentials during chlorination and chloramination of seawater mesocosms AOM was investigated. All chlorination and chloramination reactions were performed after dilution of the filtered (0.7 μm) samples to the same DOC concentration (1.5 mg-C/L) with synthetic seawater. 5 mg/L as Cl_2 of chlorine or monochloramine was added. Chlorination and chloramination experiments were conducted for 72h at pH 8.

3.1.1 Characteristics of seawater mesocosms algal bloom AOM

Table 6 shows the DOC, TN and SUVA values of the four different samples before and after dilution with synthetic seawater. Because of the different growth media with various nutrient types and concentrations, algae cell numbers within the four samples were different (data not shown), which could further lead to the different amounts of EOM and IOM giving different DOC and TN contents. Low SUVA values indicate a low aromatic character.

Bromide and iodide concentrations were not analyzed. However, bromide (synthetic seawater: 880 μmol/L) was in excess over chlorine (70.4 μmol/L) in all of the solutions during the oxidation reaction.

Table 6. DOC, TN and SUVA values of four seawater mesocosms AOM solutions before and after dilution with synthetic seawater

	Samples	1	2	3	4
Before dilution	DOC (mg-C/L)	2.87	1.50	3.08	1.70
	TN(mg-N/L)	0.322	0.15	0.38	0.10
	SUVA ($L.mg^{-1}.m^{-1}$)	1.93	0. 87	1.73	0.67
After dilution (calculated based on dilution factor)	TN (mg-N/L)	0.17	0.15	0.19	0.09

3.1.2 DBPs results

Figure 9 shows the DBPs formed during chlorination and chloramination of mesocosms AOM. Chlorination formed more THMs, HAAs, HANs and HAcAms than chloramination. As expected, bromoform was the main THMs species. During chlorination of seawater, free chlorine (HOCl) quickly reacts with bromide ions in excess to form HOBr (Equation 4). The high reactivity of HOBr with organic matter leads to the formation of brominated DBP species, especially bromoform (TBM). The highest amount of bromoform (323.8 µg/mgDOC) was detected from the chlorination of sample 2.

As expected, more HAAs were produced by chlorination (17.8-25.0 µg/mgDOC) than by chloramination (4.0-9.3 µg/mgDOC) for all samples. Monochloramine is known to form less THMs and HAAs as compared to chlorine. DBAA was the main product among all detected HAAs. Its concentration was reduced from (10.5-14.8 µg/mgDOC) by chlorination to (4.2-3.6 µg/mgDOC) by chloramination. Higher formation of trihalogenated HAAs (TCAA, DBCAA and TBAA) were detected from chlorination

(5.2-6.3 µg/mgDOC), as compared to chloramination (0.2-0.3 µg/mgDOC), also indicating the strong substitution ability of HOBr formed during the chlorination process.

DON has been associated with the formation of N-DBPs (Westerhoff and Mash 2002, Yang et al. 2007). More HANs and HAcAms were formed by chlorination (1.2-10.8 and 8.6-16.1 µg/mgDOC, respectively) than by chloramination (0.8-2.6 and 2.1-6.3 µg/mgDOC, respectively), inferring the importance of organic nitrogen incorporation from AOM. In comparison, the reactivity of monochloramine and the incorporation of inorganic nitrogen from monochloramine were significantly lower.

During the chlorination process, sample 4 exhibited similar amounts of HAAs and HAcAms to other samples, however, no bromoform was detected and much less (dibromoacetonitrile) DBAN was formed. This solution had the same DOC concentration (1.5 mg-C/L) as other samples, but had the lowest TN concentration (0.09 mg/L). The lower concentration of nitrogen-containing organic compounds may explain the lower formation of HANs. Besides, the sample 4 had the lowest SUVA value (0.67), which may explain the very low THM formation.

CIAcAm (2.8-4.0 µg/mgDOC) was detected in both chlorinated (sample 1 and 3) and chloraminated samples (sample 1 and 2). Iodinated HAcAms were reported as highly toxic (Plewa et al. 2008).

I-THMs ($CHBr_2I$, $CHBrI_2$ and CHI_3) were also detected, though only during chloramination (Figure 10). Both chlorine and chloramine rapidly oxidize I^- to HOI, however, chlorine can further oxidize the HOI to IO_3^- (Bichsel and Von Gunten 2000, Hua and Reckhow 2007). The lower oxidation power of monochloramine is not sufficient

to oxidize HOI to IO_3^-. As a result, the formation of iodinated DBPs from the reaction between HOI and organic matter is more prevalent during chloramination of waters containing iodide ion. It could be also critical during the chlorination of seawater with insufficient chlorine dosage, because insufficient chlorine would react with ammonia and organic-N from AOM to produce monochloramine and organic chloramines. These chloramines would further react with iodide ion to form HOI and ultimately iodinated DBPs.

a)

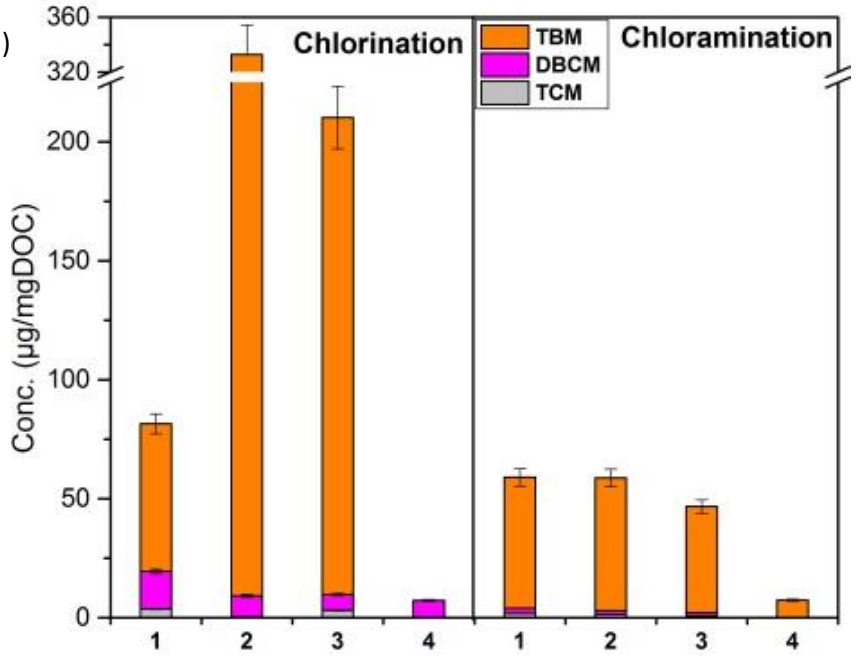

b)

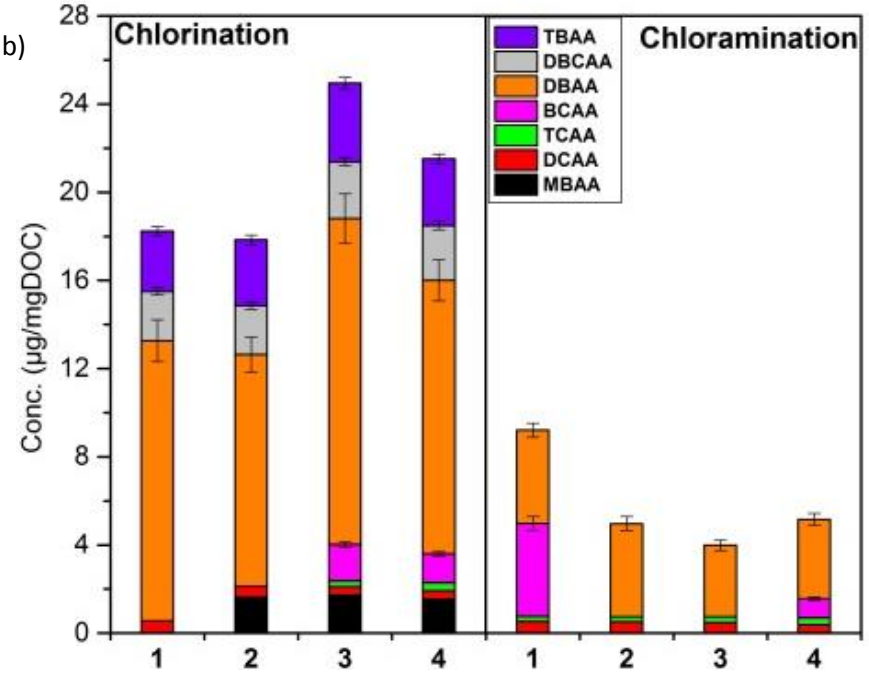
Chlorination
Chloramination
TBAA
DBCAA
DBAA
BCAA
TCAA
DCAA
MBAA
Conc. (µg/mgDOC)
0
4
8
12
16
20
24
28
1
2
3
4
1
2
3
4

c)

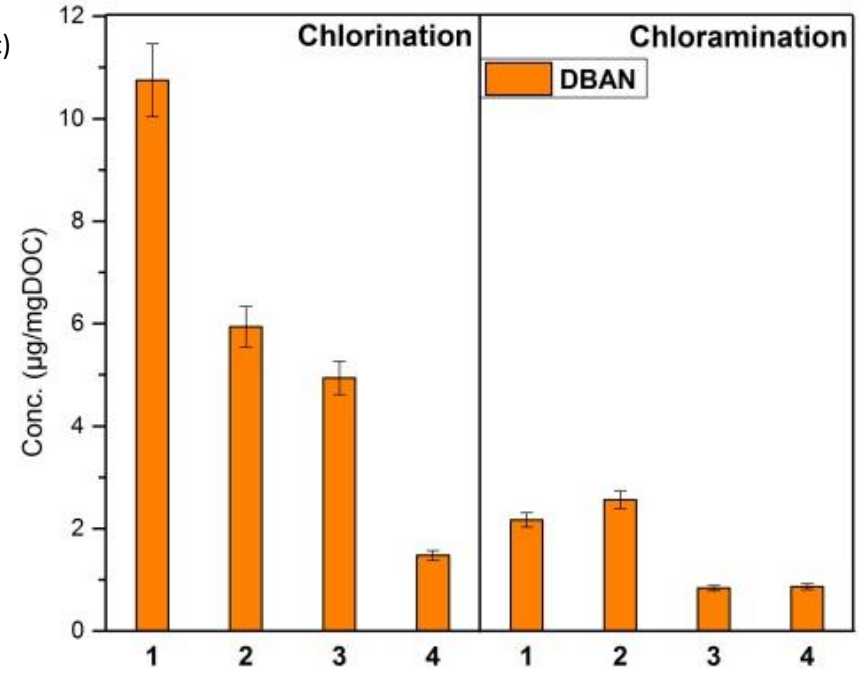
Chlorination
Chloramination
DBAN
Conc. (µg/mgDOC)
0
2
4
6
8
10
12
1
2
3
4
1
2
3
4

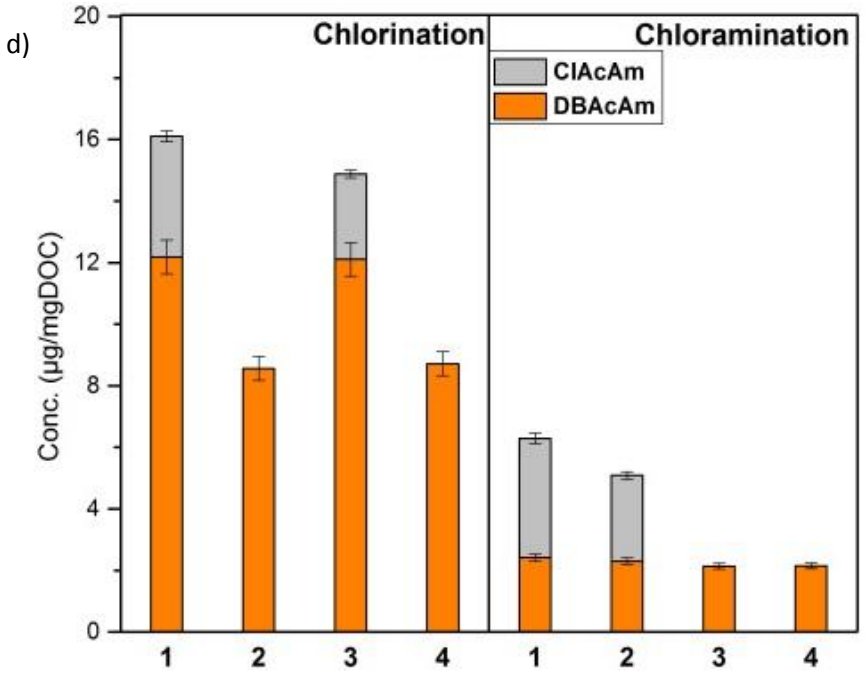

Figure 9. Formation of a) THMs, b) HAAs, c) HANs, d) HAcAms from chlorination and chloramination of four seawater mesocosms AOM, 1.5 mg-C/L, 5 mg/L as Cl_2, pH 8, 72h, 20 ^oC

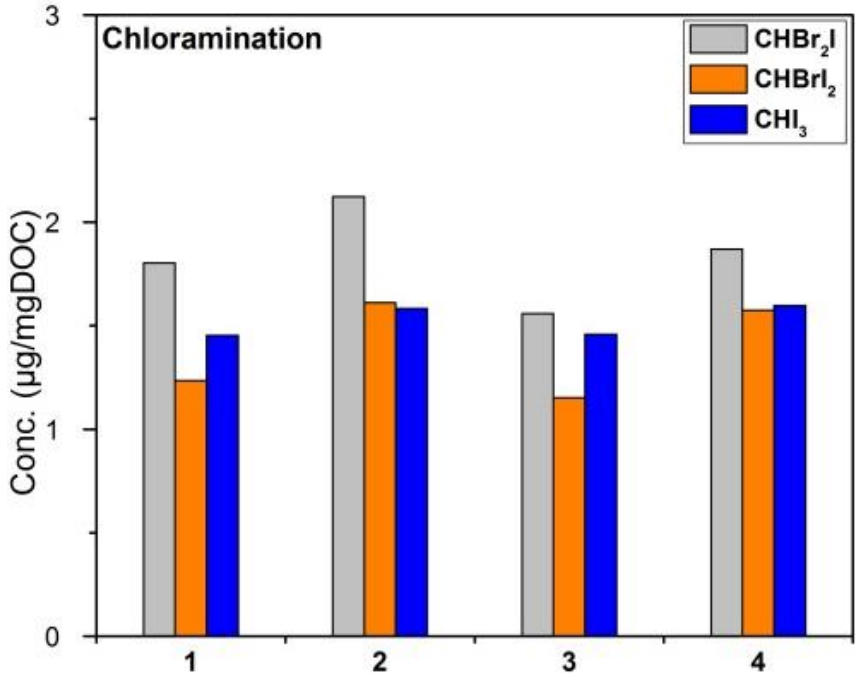

Figure 10. Formation of I-THMs from chloramination of four seawater mesocosms AOM, 1.5 mg-C/L, 5 mg/L as Cl_2, pH 8, 72h, 20 ^oC

3.2 DBPs formation from a *Trichodesmium* sp. algal bloom AOM

DBPs formation potential tests of a red tide sample, which was identified as a *Trichodesmium* sp. algal bloom, were conducted. This red tide occurred on the Red Sea coast of Saudi Arabia near the city of Yanbu during May 2013. The obtained sample was in death phase when the oxidation experiments were conducted. IOM was already released from algae cells. Samples were filtered through 0.7 µm and diluted with synthetic seawater. Chlorination and chloramination experiments were conducted for 72h at pH 8. The initial DOC value was 5 mg-C/L. The initial chlorine/monochloramine was 15 mg/L as Cl_2.

3.2.1 Characteristics of the *Trichodesmium* sp. algal bloom AOM

As compared to seawater mesocosms AOM, the *Trichodesmium* sp. AOM had much higher concentrations of DOC and TN (Table 7). Low SUVA value indicated a low aromatic character.

Table 7. DOC, TN and SUVA values of *Trichodesmium* sp. AOM after 0.7µm filtration

DOC (mg-C/L)	TN (mg/L)	SUVA ($L.mg^{-1}.m^{-1}$)
531.6	92.8	0.58

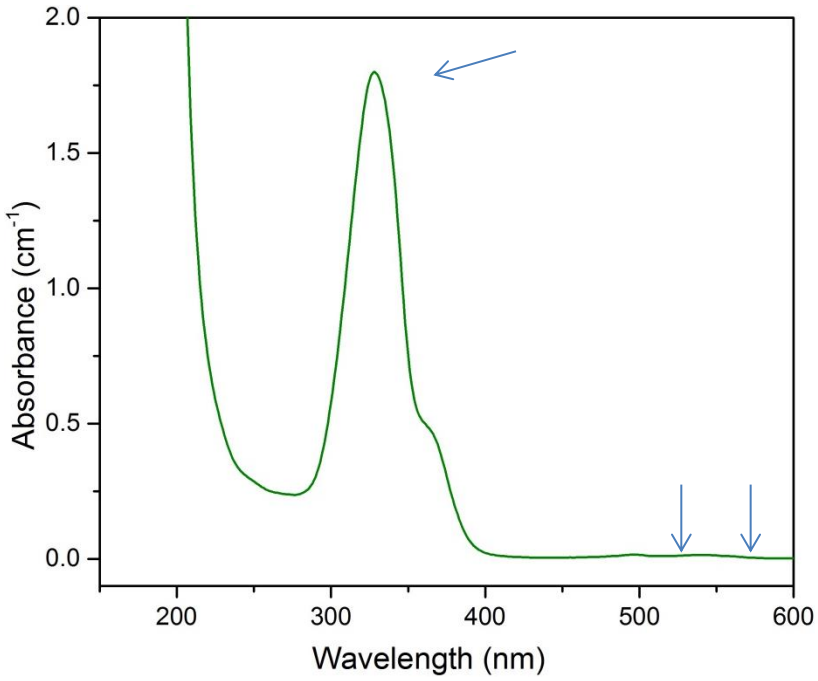

Figure 11. The UV-Vis absorbance of *Trichodesmium* sp. AOM sample (50mg-C/L, DOC)

Figure 11 presents the UV-Vis absorbance of *Trichodesmium* sp. AOM sample with 50 mg-C/L of DOC. There was a high absorbance (1.800 cm^{-1}) at 328 nm. Two lower absorbance were detected at 496 (0.015 cm^{-1}) and 542 (0.014 cm^{-1}), which corresponded to the Ex/Em wavelength pairs of 543/572 in fluorescence EEM spectra (see below).

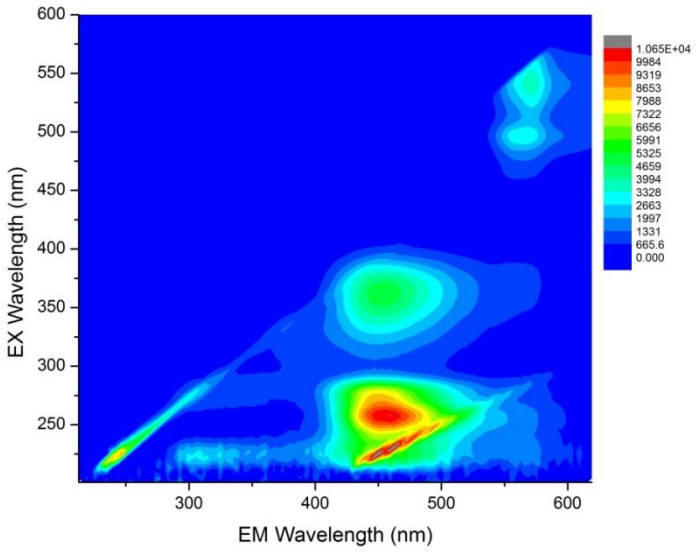

Figure 12. Fluorescence EEM spectra of *Trichodesmium* sp. AOM in synthetic seawater (5 mg-C/L, DOC)

Figure 12 shows the fluorescence EEM spectra of the *Trichodesmium* sp. AOM in synthetic seawater with DOC value of 5 mg-C/L. High concentration of salts in synthetic seawater could result in the shift of fluorescence within low excitation wavelengths. Thus, the fluorescence EEM spectra didn't exactly correspond to the UV absorbance shown in Figure 11.

The highest signal was observed at Ex/Em wavelength pairs of 258/456 nm in the domain attributed to fulvic-like compounds (Chen et al. 2003). An important signal was also detected at Ex/Em wavelength pairs of 360/453 nm, in a region where humic-like compounds are represented. No signal was detected in the protein-like region. Another high signal was exerted at Ex/Em wavelength pairs of 543/572 attributable to the strong pink/red color of *Trichodesmium* sp. algal bloom.

3.2.2 Chlorination and chloramination of *Trichodesmium* sp. algal bloom AOM

DBPs formation potential tests were conducted on the *Trichodesmium* sp. algal bloom AOM at 1h and 72h of reaction time with chlorine and monochloramine. The initial DOC concentrations were 50 mg-C/L and 5 mg-C/L, respectively. 15 mg/L as Cl_2 of chlorine or monochloramine was used.

3.2.2.1 Chlorine demand

Table 8 shows the chlorine and chloramine demands after 1h and 72h oxidation. Chlorine was consumed rapidly during the first 1h of reaction, which agrees with the higher decreases on UV-Vis absorbance and Fluorescence EEM spectra during chlorination (see below). Monochloramine demand was much lower than chlorine demand at 1h. However, most of chlorine and monochloramine were consumed after 72h. Modelling chloramines decay in the presence of 60 mg/L of bromide and in the absence of organic matter confirmed the total consumption of monochloramine after 72h (simulation performed with COPASI software). Monochloramine decay is mainly due to its auto-decomposition and not to its reaction with DOC. However, simulation of chlorine decay in the presence of 60 mg/L indicated the formation of HOBr, which remains quite stable even after 72h. Hence, the high chlorine demand observed (Table 8) after 1h and 72h can be attributed to the reactivity of HOCl/HOBr with DOC.

Table 8. Chlorine and chloramine demands during 1h and 72 chlorination/chloramination, 15mg/L as Cl_2, initial DOC: 50 mg-C/L (1h) and 5 mg-C/L (72h)

	1h chlorination	1h chloramination	72h chlorination	72h chloramination
Chlorine/chloramine demand (mg/L as Cl_2)	11.2	3.1	13.0	13.5

3.2.2.2 Effect on UV and fluorescence

UV-Vis absorbance before and after 1h oxidation (data not shown) indicated more important decreases of the peaks at 328 nm, 496nm and 542nm after 1h chlorination as compared to chloramination.

The fluorescence EEM spectra of *Trichodesmium* sp. AOM after 1h oxidation (data not shown) showed the intensity of the fluorophore corresponding to the red color (Ex/Em 543/572) decreased significantly during chlorination indicating the removal of compounds responsible for the red color. Chloramination was less efficient to reduce the red color. The intensity of signals from humic-like region and fulvic-like region reduced to some extent as compared to the initial sample, but did not show any significant differences between chlorination and chloramination. However, after 72 h oxidation, all of those fluorescence peaks were removed (data not shown).

3.2.3 DBPs results

Formation of DBPs was monitored after 1h and 72 h oxidation (Figure 13). As it can be expected, the total DBPs concentration was higher after 72 h than after 1 h. The main DBPs formed after 1h chlorination were brominated DBPs (TBM, DBAA, DBAN and DBAcAm). For chlorination process, bromoform was always the main DBP species, which was 2.2 and 241.7 µg/mgDOC within 1h and 72, respectively. Chloroform was the

main DBP species during the 1h chloramination, with a concentration of 0.34 µg/mgDOC. Again, bromoform had the highest concentration among all DBPs after 72h chloramination, with a concentration of 39.2 µg/mgDOC.

Chlorinated DBPs (TCM, DCAA and DCAcAm) were the main products with low concentration during 1h chloramination. Bromamines species (e.g., bromochloramine) formed from monochloramine and bromide ion were probably not as reactive as monochloramine or their concentration was very low within 1h. Moreover, some reactive sites of AOM could compete with bromide ion by reacting faster with monochloramine to produce chlorinated DBPs.

During 1h reaction, the DBAN formed from chlorination (1.0 µg/mgDOC) was higher than that from chloramination (0.05 µg/mgDOC). However, the concentration of DBAN after 72h chloramination (5.0 µg/mgDOC) was higher than that by 72h chlorination (2.1 µg/mgDOC), suggesting the different reaction rates of chlorine and monochloramine with AOM. The slow incorporation of inorganic nitrogen from haloamines could explain this difference (see below).

After 72h chlorination, the concentration of total HAcAms (23.8 nmol/mgDOC) was higher than that of total HANs (11.9 nmol/mgDOC). Similar result was found from the chloramination of wastewater, algal EPS and humic acid model NOM (Huang et al. 2012). Based on this result and experiments using isotopically-labeled monochloramine (^{15}N-NH_2Cl), they concluded that the formation pathways of HAN and HAcAm could be different. Further, after 72 h chlorination, DCAcAm accounted for 30% of total HAcAms, but no DCAN was detected. As proposed by Reckhow et al. (2001), HAcAm can be

formed by the hydrolysis of HANs. In this study, DCAcAm formation in the absence of DCAN could be explained by the hydrolysis of DCAN to DCAcAm. Hence, these results don't allow to conclude if the formation pathways of HANs and HAcAms are different.

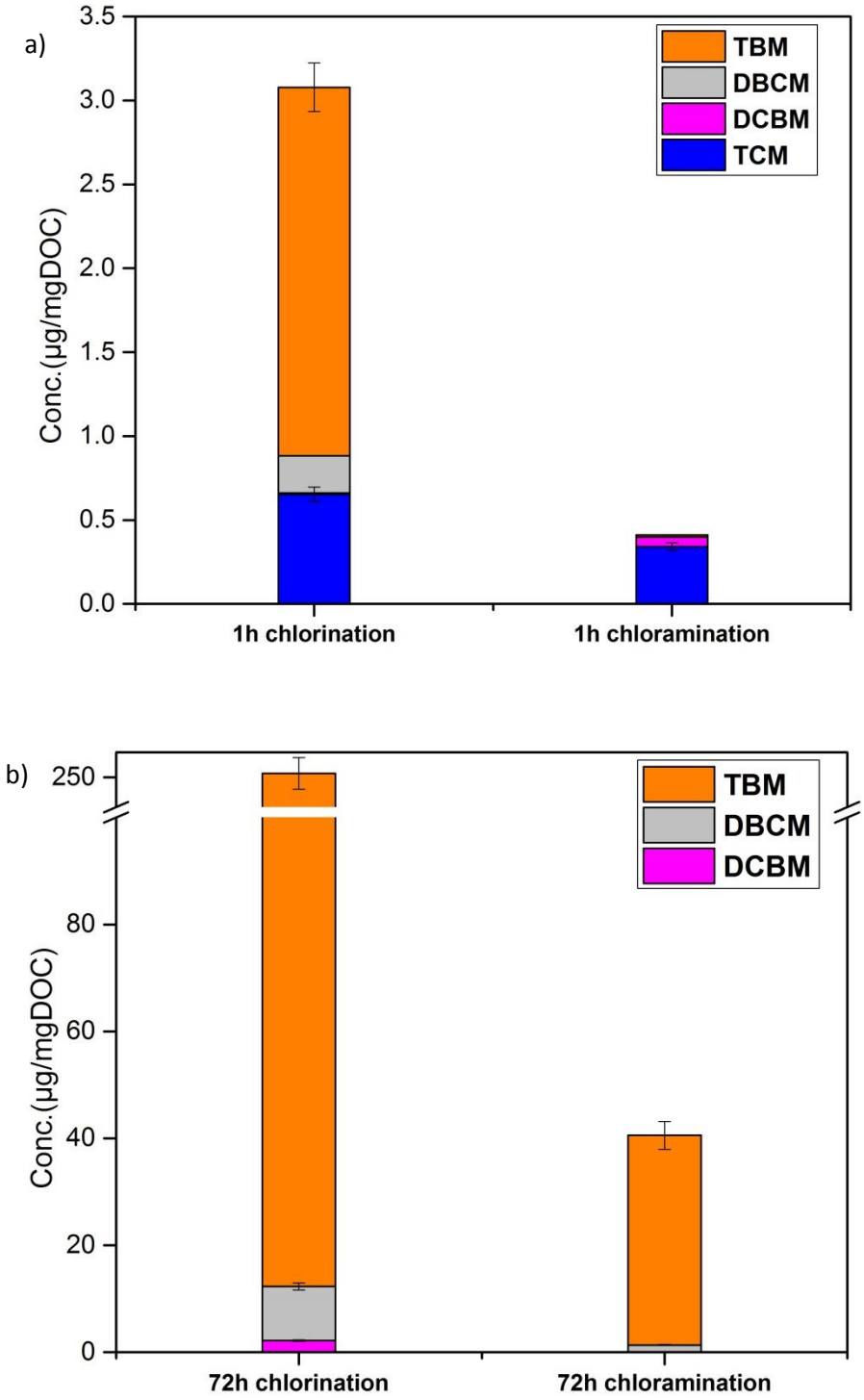

c)

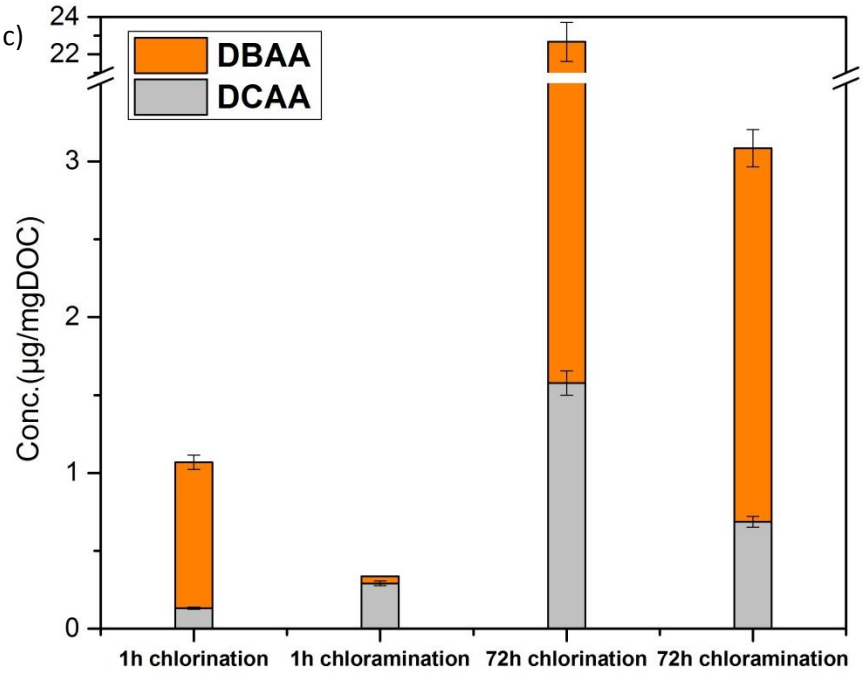
DBAA
DCAA
Conc.(µg/mgDOC)
24
22
3
2
1
0
1h chlorination
1h chloramination
72h chlorination
72h chloramination

d)

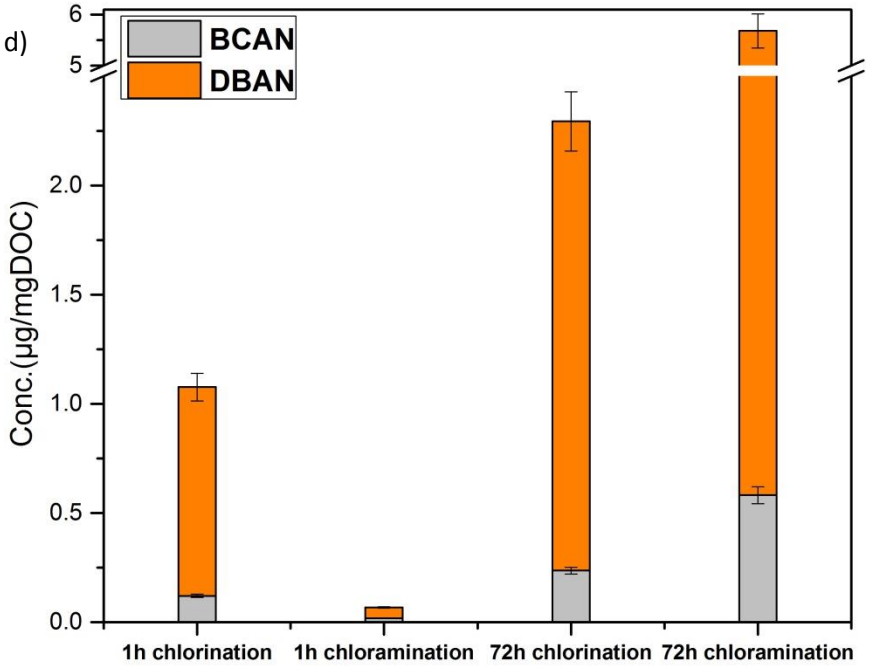
BCAN
DBAN
Conc.(µg/mgDOC)
6
5
2.0
1.5
1.0
0.5
0.0
1h chlorination
1h chloramination
72h chlorination
72h chloramination

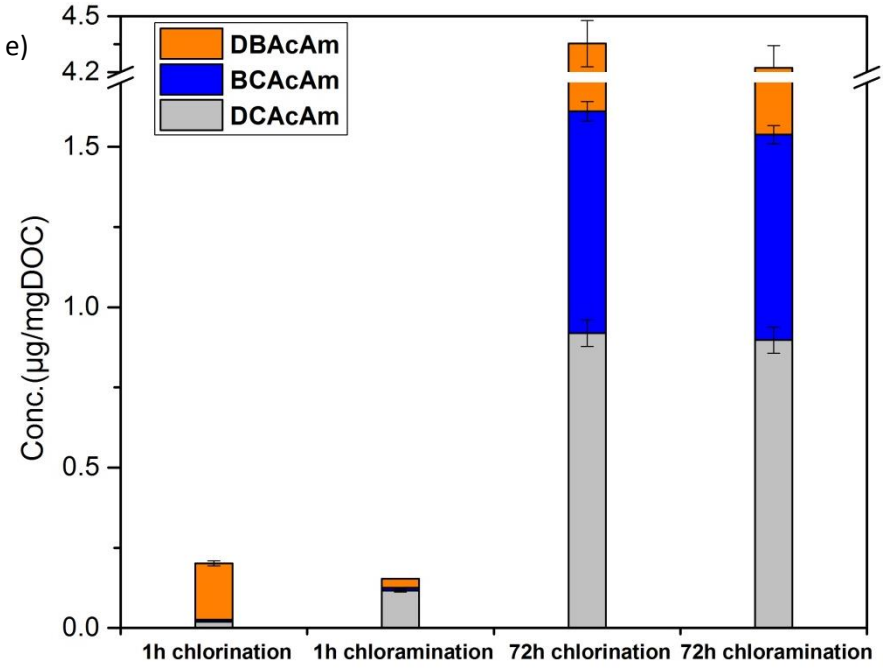

Figure 13. Formation of a) THMs (1h), b) THMs (72h), c) HAAs, d) HANs and e) HAcAms from chlorination and chloramination of *Trichodesmium* sp. algal bloom AOM during 1h (50mg-C/L, 15mg/L as Cl_2) and 72h reaction time (5 mg-C/L, 15mg/L as Cl_2), pH 8, 20 ^{o}C

3.2.4 Exploration of nitrogen source in N-DBPs

Chloramination experiments were conducted on the *Trichodesmium* sp. algal bloom AOM sample using isotopically-labeled monochloramine (^{15}N-NH_2Cl) in order to investigate the source of nitrogen in N-DBPs (i.e., HANs and HAcAms). About 50% of DBAN, DBAcAm and BCAcAm originated from monochloramine (Figure 14), indicating the importance of inorganic nitrogen incorporation during AOM chloramination. This result is consistent with previous studies on drinking water influent, NOM and algal EPS (Huang et al. 2012). No ^{15}N-DCAcAm and ^{15}N-BCAcAm were detected. This may be due to the low levels of concentration observed for these DBPs (DBAcAm was the major HAcAms species detected), thus ^{15}N-analogues of these products were probably below the detection limit and could not be easily quantified.

As shown in Figure 13 d) and e), after 72h reaction time, chloramination produced more HANs (5.7 µg/mgDOC) than chlorination (2.3 µg/mgDOC). Moreover, similar amounts of HAcAms were formed from chlorination (4.4 µg/mgDOC) and chloramination (4.3 µg/mgDOC). However, almost 50 % of DBAN, DBAcAm and BCAN produced during chloramination were coming from monochloramine. These results indicated that although chloramines are less reactive with nitrogenous organic compounds as compared to chlorine, they can produce the same or even higher amount of N-DBPs than chlorine through the incorporation of inorganic nitrogen.

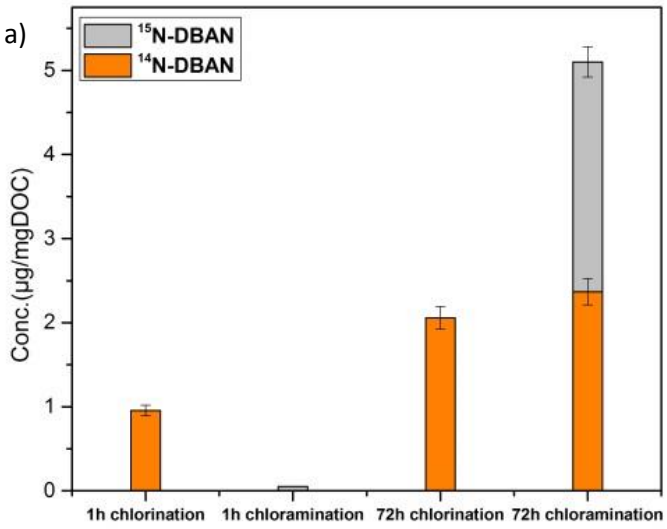

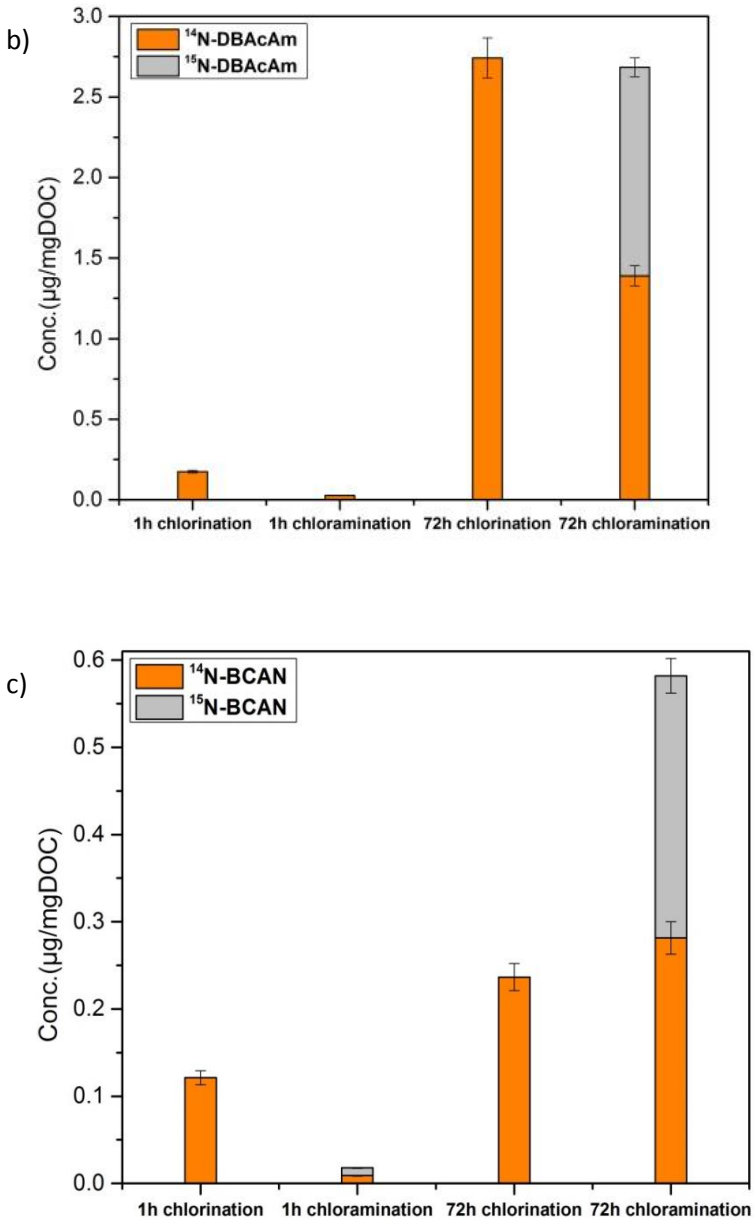

Figure 14. a) ^{15}N-DBAN, b) ^{15}N-DBAcAm and c) ^{15}N-BCAN formation from chlorination and chloramination of *Trichodesmium* sp. algal bloom AOM during 1h reaction time (50mg-C/L, 15mg/L as Cl_2) and 72h reaction time (5 mg-C/L, 15mg/L as Cl_2), pH=8, 20 ^{o}C

3.3 DBPs formation from *Hymenomonas* sp. AOM

3.3.1 Characteristics of *Hymenomonas* sp. AOM

Hymenomonas sp. monoculture was studied as AOM source during chloramination. Samples were collected at different growth phases (exponential phase, stationary phase and death phase). As shown in Table 9, total organic carbon (TOC) increased during the growth phase due to the increasing biomass production. This agrees with previous studies on diatom and blue-green algae (Nguyen et al. 2005) and *Microcystis aeruginosa* (Huang et al. 2009). Dissolved organic carbon (DOC) values (after filtration through 0.7 μm) were significantly lower because of the removal of large colloidal organic matter and algae cells. Total nitrogen concentration (TN) in exponential phase was the highest, because of the presence of inorganic nitrogen coming from nutrient media (i.e., NO_3^-). The organic nitrogen concentration was not analyzed, but it is known that the protein and organic nitrogen levels decrease with age of culture (Brown et al. 1993). This is consistent with the fluorescence of region IV in EEM data (Figure 8),exhibiting a lower signal in the protein-like region (region IV) during stationary phase and death phase as compared to exponential phase. The TN difference between filtered and unfiltered sample was due to the removal of organic nitrogen during 0.7 μm filtration.

Table 9.TOC and TN values of different growth phases

	Exponential phase	Exponential phase 0.7 µm filtration	Stationary phase	Stationary phase 0.7 µm filtration	Death phase 0.7 µm filtration
TOC (mg-C/L)	20.9	3.9	92.4	16.4	25.4
TN (mg-N/L)	8.83	7.62	3.97	0.89	0.96

Figure 15 shows the FEEM spectra for *Hymenomonas* sp. in exponential, stationary and death phase. The highest signal was located in region I and region II, which are attributed to aromatic proteins (e.g., tyrosine, tryptophan) (Chen et al. 2003). A different EEM spectrum was obtained from *Trichodesmium* sp. algal bloom sample (Figure 12), since *Trichodesmium* sp. was mainly enriched in humic-like and fulvic-like compounds (region III and V). Fluorophores in region III and V were also detected from *Hymenomonas* sp. samples. Region IV exhibited a lower signal during stationary phase and death phase as compared to exponential phase, indicating a lower presence of protein-like compounds. This result is similar to previous fluorescence EEM spectra obtained from EOM of C. vulgaris in exponential phase (Henderson et al. 2008). *Hymenomonas* sp. in death phase exerted higher fluorescence signal in region V than other growth phases, suggesting the presence of humic-like compounds in higher concentration in the EOM.

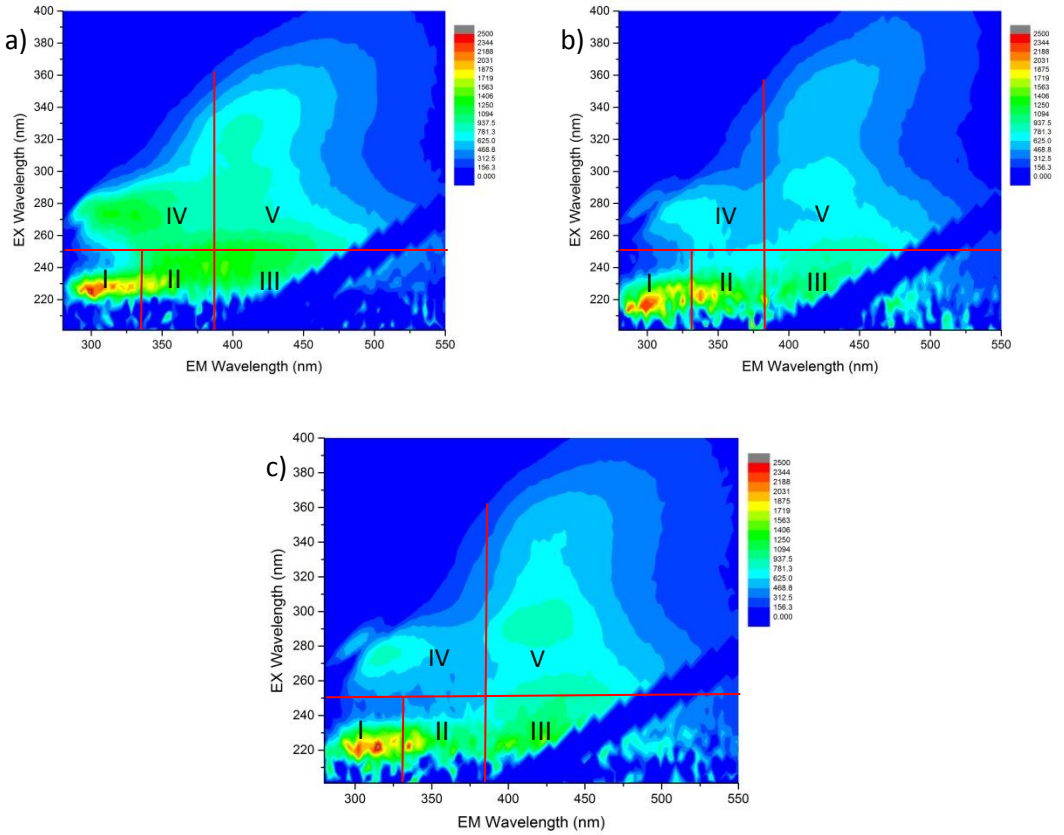

Figure 15. Fluorescence EEM spectra for *Hymenomonas* sp. in a) exponential, b) stationary and c) death phase, 5 mg-C/L of DOC, 0.7µm filtration

3.3.2 DBPs results

Effect of algae growth phase on DBPs formation was studied by chloraminating (^{15}N-NH_2Cl) samples for 72 h. Samples were first filtered through 0.7µm filter, and then diluted with synthetic seawater to the same DOC. EOM should represent the main AOM source during exponential phase and stationary phase. Death phase contained EOM and IOM as well, which was released from cells.

DBPs formation was different among these three growth phases (Figure 16). Total THMs concentration increased from exponential phase to death phase. Similar results from chlorination of *Microcystis aeruginosa* has been reported (Fang et al. 2010a). Bromoform

was the main THMs species, because of the presence of 880 µmol/L of bromide ion in synthetic seawater. The highest concentration of bromoform (81.2 µg/mgDOC) was detected in the sample collected during death phase. However, the death phase exhibited the lowest HAAs concentration (0.76 µg/mgDOC), suggesting that the IOM in death phase favors THMs formation over HAAs formation. Similar results have been reported for microcystis (Huang et al. 2009). The formation of ^{14}N-DBAN that originated from organic nitrogen was similar among all phases (i.e., 2 µg/mgDOC). However, much higher formation of ^{15}N-DBAN (9.5 µg/mgDOC) was detected from the death phase. As described above, *Hymenomonas* sp. in death phase had more humic- like compounds, but less protein-like compounds. Larger formation of ^{15}N-DBAN from the death phase seems to indicate the higher reactivity of humic- like compounds (i.e., enriched in aromatic compounds) with monochloramine, leading to higher inorganic nitrogen incorporation (see part 3.5).

As expected, the highest amount of ^{14}N-DBAcAm (4.7 µg/mgDOC) was produced from the sample in exponential phase because of the presence of higher concentration of organic nitrogen-containing compounds. Besides, no ^{15}N-DBAcAm was detected from exponential phase. ^{15}N-DBAcAm was detected in the stationary phase (1.5 µg/mgDOC) and the death phase (2.1 µg/mgDOC), exhibiting a slight increase. The highest DBAN formation and DBAcAm formation were found in death phase and exponential phase, respectively, suggesting different formation pathways for HANs and HAcAms.

a)

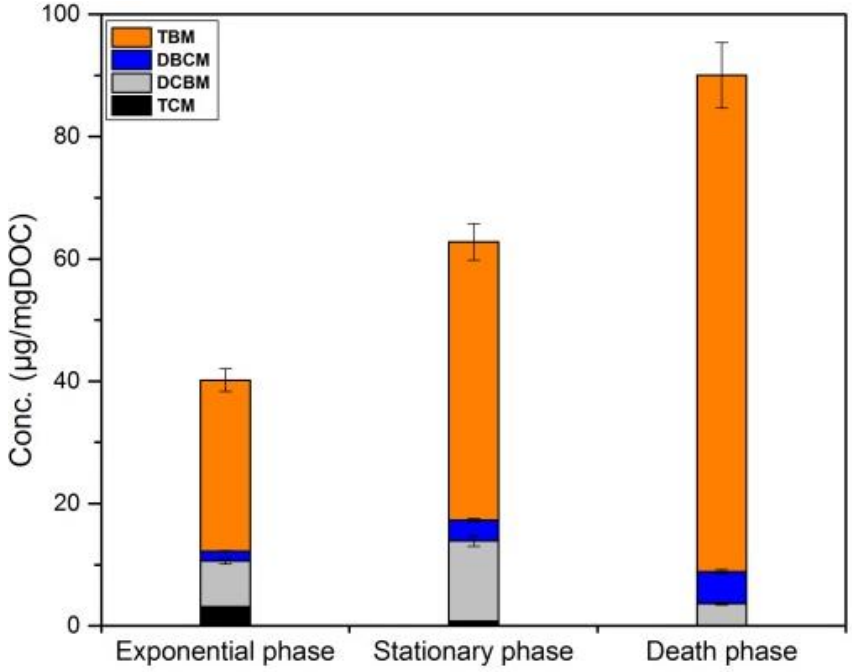
TBM
DBCM
DCBM
TCM
Conc. (µg/mgDOC)
0
20
40
60
80
100
Exponential phase
Stationary phase
Death phase

b)

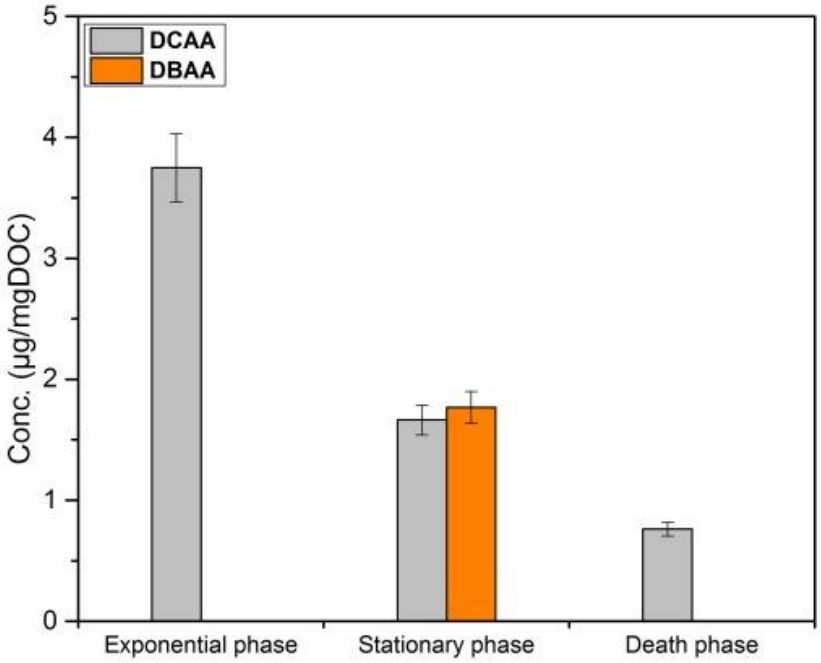
DCAA
DBAA
Conc. (µg/mgDOC)
0
1
2
3
4
5
Exponential phase
Stationary phase
Death phase

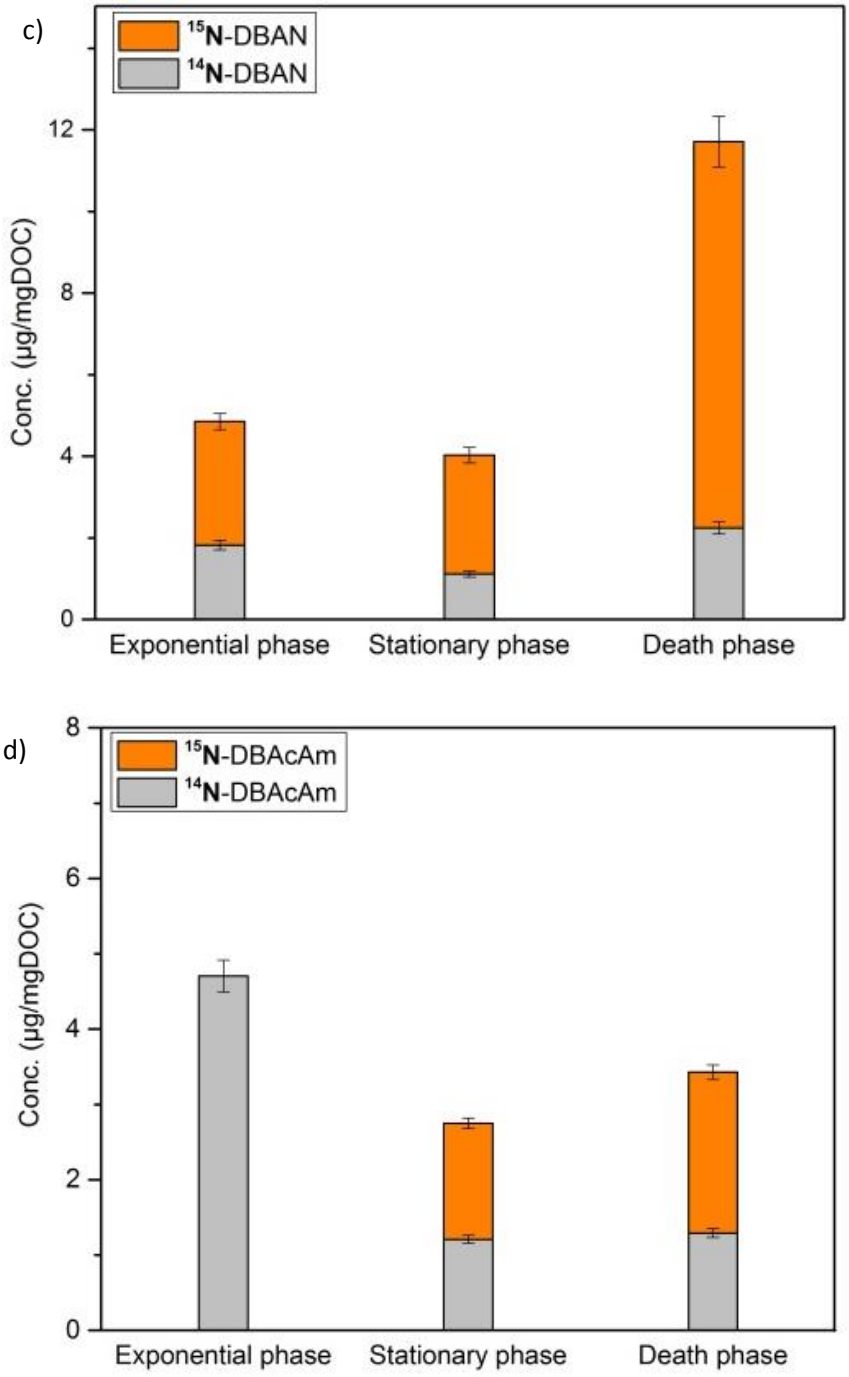

Figure 16. a) THMs, b) HAAs, c) DBAN and d) DBAcAm formation from chloramination of *Hymenomonas* sp. in exponential (DOC: 1.5mg-C/L, chloramine: 5 mg/L as Cl_2), stationary (DOC: 5mg-C/L, chloramine: 15 mg/L as Cl_2) and death phase (DOC: 5mg-C/L, chloramine: 15 mg/ L as Cl_2),pH 8, 72 h, 20 ^{o}C

3.4 DBPs formation from amino acids

As shown in Figure 12, *Hymenomonas* sp. was enriched in protein-like, tryptophan-like and tyrosine-like compounds, which are made up of amino acids. Generally, proteins and amino acids are important AOM fractions (Nguyen et al. 2005). Her et al. (2004) reported that blue-green algae contained 68% of proteins. However, the free amino acids from *Microcystis aeruginosa* comprised only 2.5% of TON (Fang et al. 2010b). Besides, only 6% of total amino acids in source waters are free amino acids (Dotson and Westerhoff 2009).

Though free amino acids are present in water in low concentration, their stuctures and functional groups affect the reactivity of proteins and peptides. Previous studies found that amino acids exhibit high chlorine demand and contribute to the HAAs, THMs and N-DBPs formation (Hong et al. 2009, Hureiki et al. 1994, Yang et al. 2010). Chu et al. (2010b) reported that amino acids are precursors of DCAcAm. However, limited studies focused on the chloramination of amino acids and their N-DBPs formation potential, especially HAcAms.

In this study, DBPs formation potential tests were conducted during chlorination and chloramination of amino acids. DBPs formation kinetics and conditions (e.g., influence of chlorine dose and pH) were investigated. Moreover, isotopically-labeled monochloramine ($^{15}N\text{-}NH_2Cl$) was used to investigate the nitrogen source and formation pathways of N-DBPs from amino acids.

In order to avoid the formation of various DBPs, no bromide was added in model compounds oxidation experiments. Moreover, except the study on pH influence, all of

experiments on model compounds were conducted in Milli-Q water at pH 7 (10 mM phosphate buffer), which was different from the previous AOM oxidation experiments in synthetic seawater at pH 8.

3.4.1 Haloacetamides formation by chlorination of 20 amino acids

20 amino acids were chlorinated individually for 72h at pH 7. The initial concentration of amino acid was 5 µmol/L. The initial chlorine concentration was 5 mg/L as Cl_2, with Cl_2/amino acid molar ratio of 14.

Results showed (Appendices:Table 10) that all of 20 amino acids were precursors of DCAcAm or TCAcAm. However, most of them formed less than 0.1 µg/L of DCAcAm and TCAcAm. Aspartic acid produced the highest DCAcAm concentration (31.9 µg/L, 5% molar yield from aspartic acid), followed by asparagine (28.9 µg/L, 4.4% molar yield). Tyrosine exhibited the highest TCAcAm (10.7 µg/L, 1.3% molar yield), followed by tryptophan (9.0 µg/L, 1.1% molar yield), asparagine (2.3 µg/L, 0.28% molar yield) and histidine (1.9 µg/L, 0.24 % molar yield). Similar results on DCAcAm formation from amino acids were obtained in previous studies (Chu et al. 2010b). The high formation potential of HAcAms from these 5 amino acids was related to their structures and functional groups. Tyrosine, tryptophan and histidine have activated aromatic rings, moreover, aspartic acid and asparagine have a carboxyl group and an amide group, respectively. This will be discussed in more details below.

3.4.2 Comparison between chlorine and chloramine reactions

The major precursors of HAcAms among amino acids (aspartic acid (Asp), asparagine (Asn), histidine (His), tyrosine (Tyr) and tryptophan (Trp)) were further studied for the

comparison between chlorination and chloramination. Chlorination and chloramination experiments were conducted for 72h at pH 7. The initial concentration of amino acid was 50 µmol/L. 50 mg/L as Cl_2 of chlorine or monochloramine was used. The Cl_2/amino acid molar ratio was 14.

a)

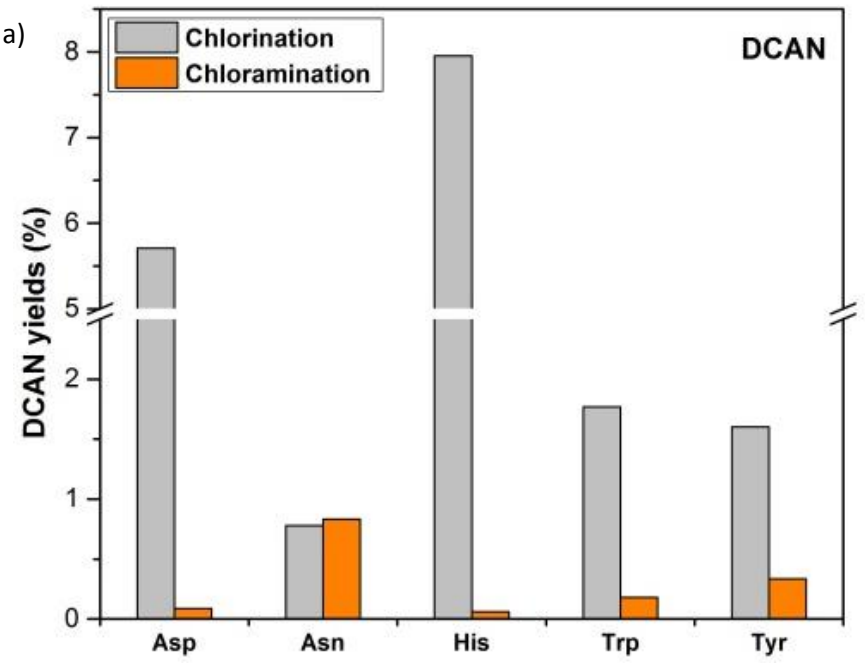

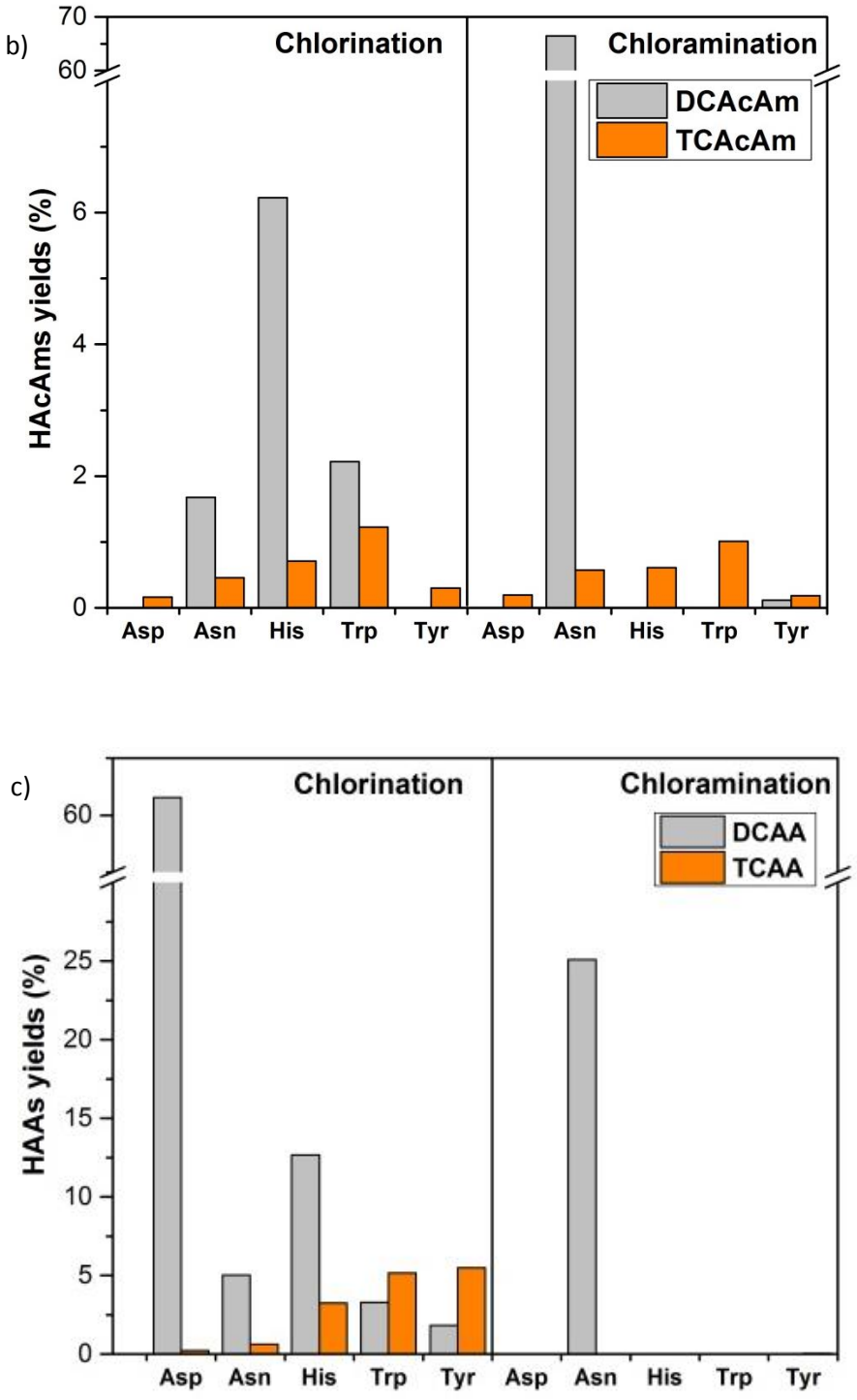

Figure 17. a) DCAN, b) HAcAms, c) HAAs formation from chlorination and chloramination of amino acids, initial amino acid: 50 µmol/L, initial chlorine/chloramine: 50 mg/L as Cl_2, pH7, 72 h, 20 ^{0}C

Figure 17 shows the DBPs formation from chlorination and chloramination of amino acids. Among all examined DBPs (HANs, HAAs and HAcAms), DCAN, DCAA, TCAA,

DCAcAm and TCAcAm were detected. DCAN formation during chlorination followed the order: histidine (8.0% molar yield), aspartic acid (5.6%), tryptophan (1.8%), tyrosine (1.6%) and asparagine (0.8%). Ueno et al. (1996) reported that histidine formed the highest DCAN during the chlorination of 20 amino acids (pH 7, Cl_2/amino acid molar ratio of 14). However, the highest DCAN formation was found from asparagine during chlorination of 20 amino acids in another study (pH 7.2, Cl_2/organic-N molar ratio of 30) (Yang et al. 2012), indicating that the chlorine dose can influence DCAN formation.

Figure 18 shows a proposed mechanism for the formation of HANs upon chlorination of α-amino acids (Yang et al. 2010). Chlorinated organic compounds are formed first due to the chlorine substitution, then after the decarboxylation and elimination processes, aldehydes and nitriles are formed.

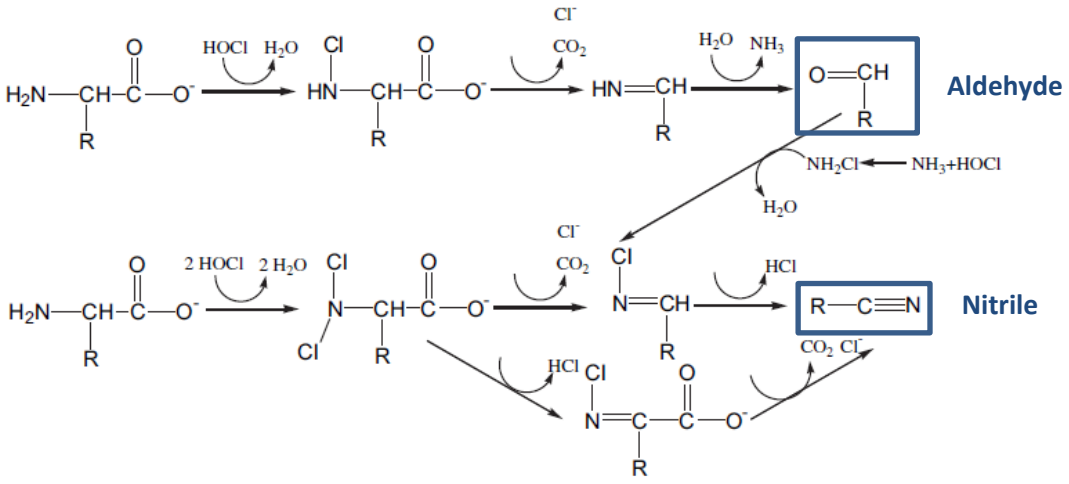

Figure 18. chlorination of α-amino acids, modified from (Yang et al. 2010)

DCAN is known to further hydrolyze to produce DCAcAm and DCAA during chlorination (Reckhow et al. 2001). The highest DCAcAm formation during chlorination

was also found from histidine. This result may confirm that DCAN and DCAcAm follow a common pathway, hydrolysis of DCAN producing DCAcAm (Reckhow et al. 2001).

Besides, TCAcAm and TCAA were detected in lower concentration during chlorination (0.2-1.2% molar yield for TCAcAm, 0.2-5.5% for TCAA). The highest TCAcAm formation was found from tryptophan (1.2 %), followed by histidine (0.7%). Tyrosine produced the highest TCAA (5.5%), followed by tryptophan (5.3%). Hence, the main precursors of TCAcAm/TCAA were not the main precursors of DCAcAm/DCAA. Reckhow and Singer (1986) have reported that TCAA and DCAA might have different precursors. There was a good correlation between TCAcAm and TCAA formation, except for tyrosine. This could be related to the hydrolysis of TCAcAm to TCAA.

The high reactivity of histidine, tyrosine and tryptophan could be related to the presence of aromatic rings in their molecular structure. Ring opening can occur during chlorination and nitrogen atoms present in tryptophan and histidine could contribute to the DCAN and HAcAms formation to a certain extent. Especially, the presence of 2 additional nitrogen atoms in the aromatic ring of histidine could explain its higher DCAN and DCAcAm formation potential. This was confirmed by experiments using ^{15}N-NH_2Cl (see part 3.4.3).

DCAN, DCAcAm and TCAcAm formation was also detected from the chloramination of amino acids. The concentration of TCAcAm formed from chloramination was similar to chlorination (0.2-1.0% molar yield). Chloramination formed less DCAN and DCAcAm than chlorination except for asparagine, producing up to 66.5% of DCAcAm (only 1.7% from chlorination). In addition, asparagine produced 25.1% of DCAA, but no DCAA was detected from the other amino acids. Huang et al. (2012) proposed a formation

mechanism to explain the DCAcAm formation from asparagine (Figure 19). DCAcAm is likely to originate from the amide group in asparagine (Table 3). However, no specific pathway for chloramination was described, since the formation of DCAcAm was similar during chlorination and chloramination in their experimental conditions (100 µmol/L of asparagine, 10 mg/L as Cl_2, pH 6.9, 2h). In our experiment (50 µmol/L of asparagine, 50 mg/L as Cl_2, pH 7, 72h), the important difference of DCAcAm formation between chlorination and chloramination could be explained by the oxidation of the amide group of asparagine by HOCl, thus reducing its potential as a DCAcAm precursor (see part 3.4.4.1).

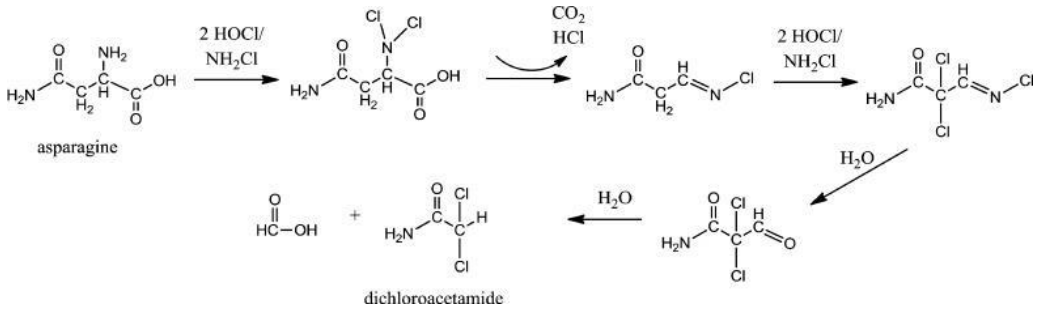

Figure 19. DCAcAm formation from asparagine (Huang et al. 2012)

3.4.3 Nitrogen source of DCAN, DCAcAm and TCAcAm

Previous studies suggested two formation pathways for HANs and HAcAms formation: the decarboxylation pathway and the aldehyde pathway (Shah and Mitch 2012, Yang et al. 2010). During the decarboxylation pathway, the nitrogen atom in HANs and HAcAms originates from organic compounds. During the aldehyde pathway, the nitrogen atom comes from monochloramine (See part 1. Literature review). Previous researchers proposed the same reaction mechanism for chloramination of α-amino acids than for

chlorination (Figure 18) (Shah and Mitch 2012, Yang et al. 2010). During the chloramination of α-amino acids, aldehydes and nitriles are produced through substitution, decarboxylation and elimination processes. Nitiles also can be formed from the aldehydes reaction with monochloramine. Hydrolysis of nitriles further leads to the HAcAms formation.

In order to investigate the nitrogen source of DCAN, DCAcAm and TCAcAm during the chloramination of amino acids, experiments were conducted using isotopically-labeled monochloramine (^{15}N-NH_2Cl). Seven amino acids were studied (asparagine, aspartic acid, histidine, phenylalanine (Phe), proline (Pro), tryptophan and tyrosine). In addition to the amine group, tryptophan and histidine contain nitrogen atoms in their structure (Table 2). Proline nitrogen atom is part of a secondary amine group while the other amino acids investigated are all primary amines. Amino acids were chloraminated using ^{15}N-NH_2Cl for 3 days at pH 7. The initial concentration of amino acid and chloramine was 250 µmol/L and 100 mg/L as Cl_2, respectively. A higher initial concentration of amino acid was used with the objective to enhance the formation of HAcAms since the previous experiment condition didn't allow the detection of HAcAms from some amino acids (see part 3.4.2). Chloramine to amino acid molar ratio was 5.6.

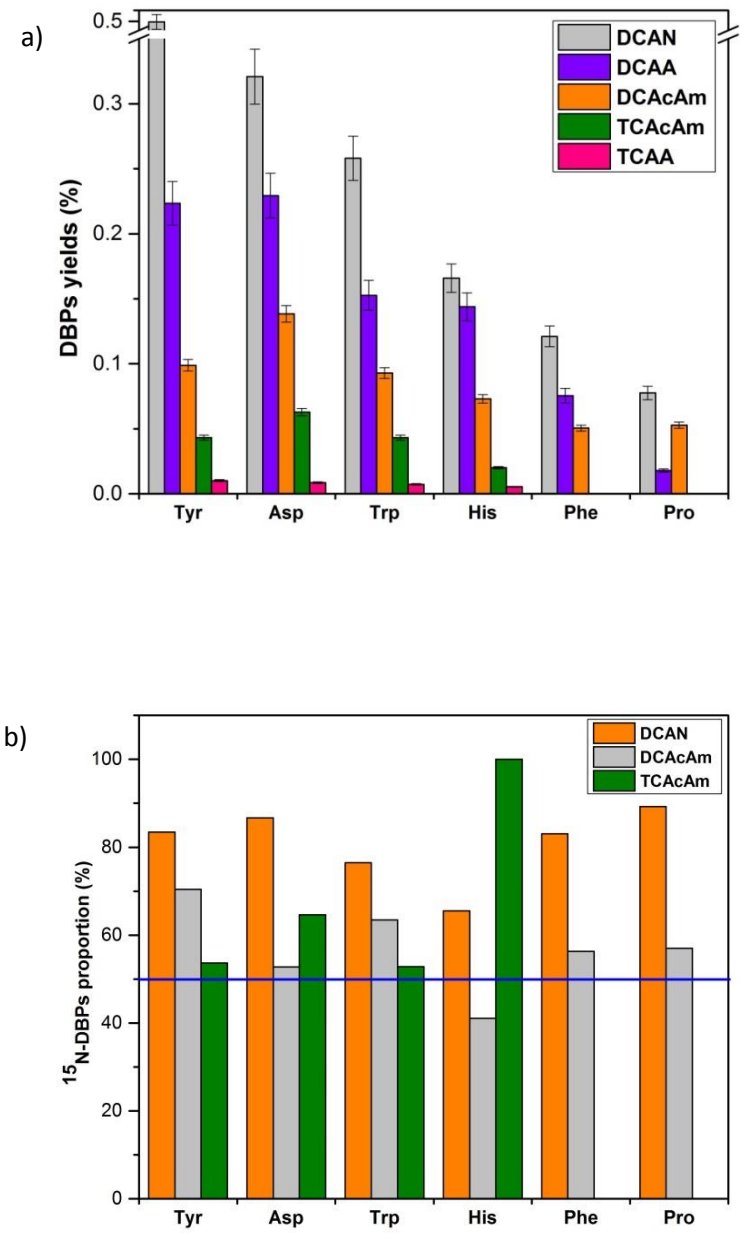

Figure 20. a) DBPs formation from chloramination of amino acids; b) ^{15}N-DBPs percentage of DCAN and DCAcAm, initial chloramine: 100 mg/L as Cl_2, initial amino acid: 250 µmol/L, pH7, 72h, 20 ^{o}C

Again, among all examined amino acids, asparagine produced the highest DCAcAm (42.4% molar yield), as already shown in part 3.4.2. Asparagine also formed the highest concentration of DCAN (3.1%) (asparagine data not shown in Figure 20).

As shown in Figure 20 a), for all of examined amino acids (except asparagine and proline), DCAN was the major DBP species formed (0.1-0.5 % molar yields), followed by DCAA (0.02-0.23%), DCAcAm (0.05-0.14%), TCAcAm (0.02-0.06%) and TCAA (0.005-0.01%). For proline, DCAN (0.08%) was higher than DCAcAm (0.05%), followed by DCAA (0.02%). It has been reported that DCAcAm could be the intermediate product when DCAN hydrolyzes to DCAA during chlorination (Reckhow et al. 2001). However, limited studies focused on the stabilities of HANs and HAcAms during chloramination. In this result, the DCAA concentration was higher than DCAcAm among all amino acids (except asparagine and proline), while the TCAA was always lower than TCAcAm. Further studies are needed to investigate the DCAcAm and TCAcAm hydrolysis products and hydrolysis rates in the presence of monochloramine.

No TCAcAm was detected from proline and phenylalanine. Proline was the lowest precursor of all DBPs among all the amino acids. This can be related to its particular structure (i.e., secondary amine).

Phenylalanine and tyrosine have similar structures. However, as compared to phenylalanine, tyrosine formed more DCAN, DCAA and DCAcAm. Besides, TCAA and TCAcAm were also produced by tyrosine, while they were not detected from phenylalanine. The higher reactivity of tyrosine than phenylalanine might be explained by the activation of its aromatic ring by the hydroxyl group (-OH). In order to elucidate the mechanisms of N-DBPs formation from chloramination of aromatics and the influence of the hydroxyl groups, phenolic compounds (i.e., phenol and resorcinol) were studied (see part 3.5).

Figure 20 b) presents the ^{15}N-DBPs proportions in total DCAN, total DCAcAm and total TCAcAm. The proportion of ^{15}N-DBPs was in general higher than 50% (except the ^{15}N-DCAcAm from histidine). This indicates that substantial part of the nitrogen originated from monochloramine, suggesting the importance of aldehyde pathway. ^{15}N-DCAcAm proportion from histidine was 41.1%, the lowest among all examined amino acids. This higher formation of ^{14}N-DCAcAms from histidine as compared to ^{15}N-DAcAms can be explained by the presence of three nitrogen atoms in the histidine molecular structure.

In general, the proportions of ^{15}N-DCAN (65-90%) were higher than that of ^{15}N-DCAcAm (40-70%), indicating a higher incorporation of inorganic nitrogen into DCAN than DCAcAm. Thus, this result suggests that the aldehyde pathway favors DCAN formation than DCAcAm formation. Moreover, if DCAcAm was produced only from the hydrolysis of DCAN, the inorganic nitrogen incorporation factor should be the same. Accordingly, an independent formation pathway for DCAcAm should exist. Different ^{15}N incorporations between DCAN and DCAcAm have also been reported during chloramination of humic acid, algal EPS and wastewater (Huang et al. 2012).

For asparagine chloramination, only 1.7% of DCAcAm nitrogen came from monochloramine. This result agrees with the previous hypothesis that amide group in asparagine plays a key role in DCAcAm formation. Besides, the ^{15}N incorporation for DCAN was 90%, indicating that DCAN formation from asparagine followed a totally different pathway than DCAcAm (.i.e., aldehyde pathway).

3.4.4 Factors influencing the formation of N-DBPs

The influence of Cl_2/amino acid molar ratio, pH and reaction time on N-DBPs formation was evaluated. Asparagine was chosen due to the high formation potential of N-DBPs from asparagine.

3.4.4.1 Influence of Cl_2/asparagine molar ratio

The influence of Cl_2 to asparagine molar ratio on DBPs formation during chlorination and chloramination was investigated. The initial concentration of asparagine was 250 μmol/L. Chlorination and chloramination experiments were conducted for 2h at pH 7. The Cl_2 to asparagine molar ratios were 1, 2, 10 and 20.

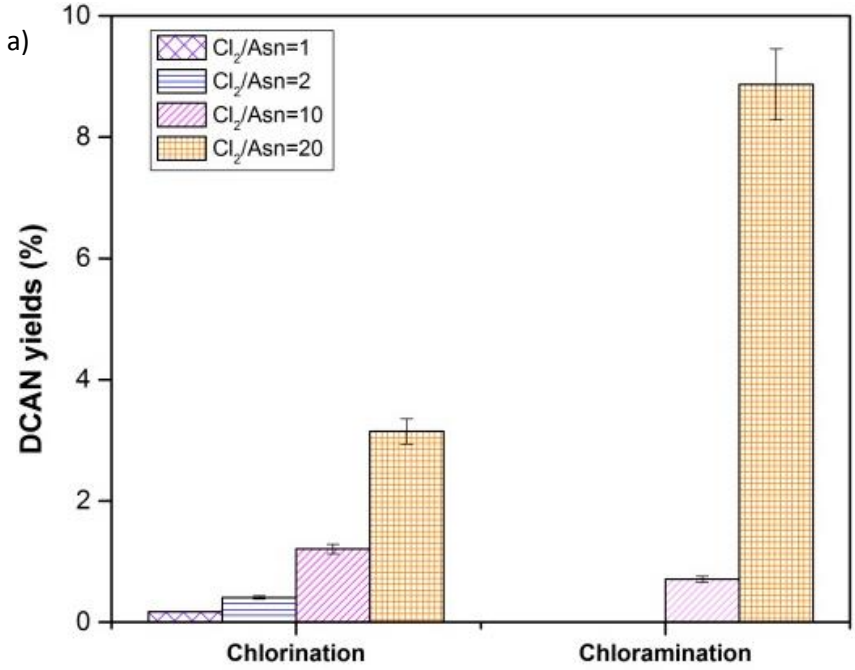

b)

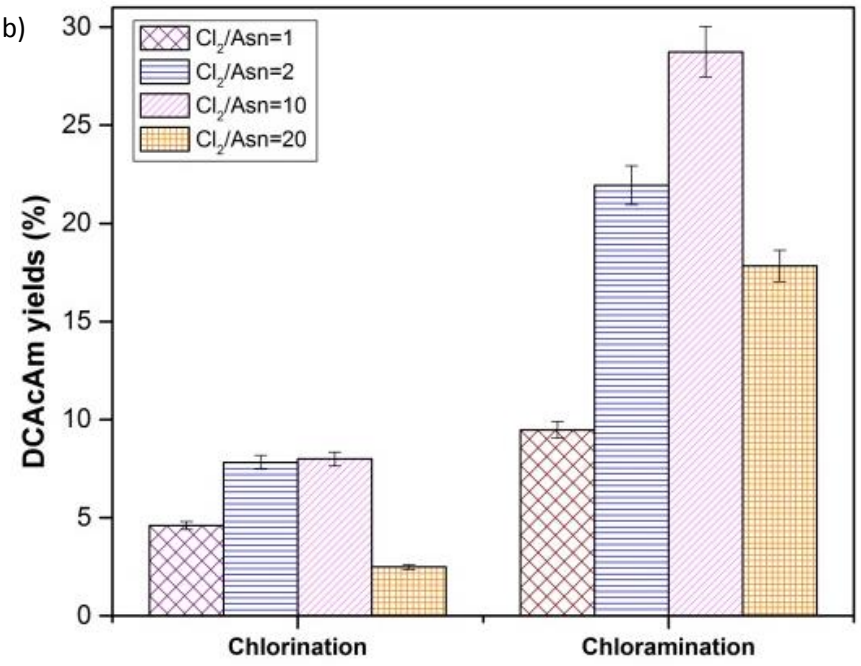
DCAcAm yields (%)
30
25
20
15
10
5
0
Cl2/Asn=1
Cl2/Asn=2
Cl2/Asn=10
Cl2/Asn=20
Chlorination
Chloramination

c)

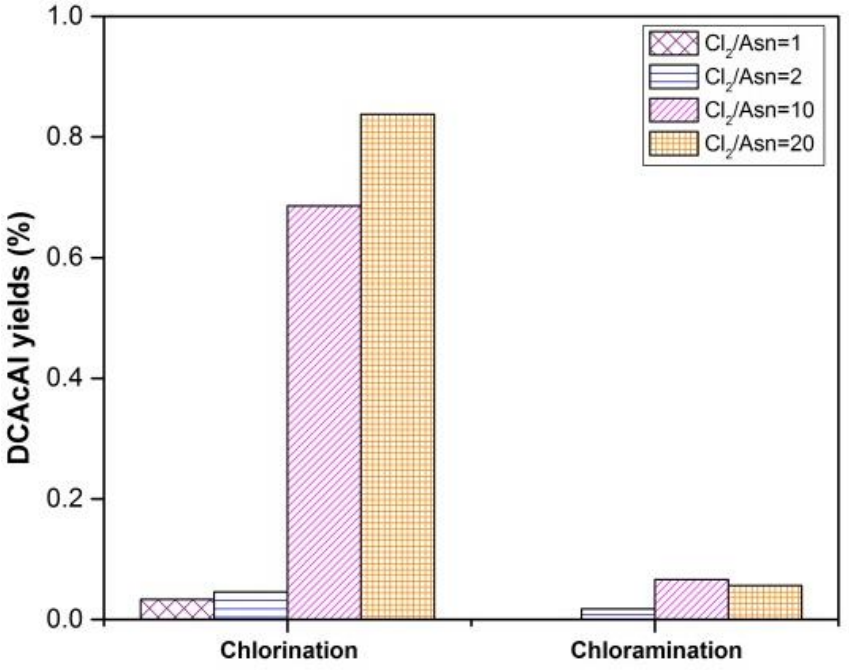
DCAcAl yields (%)
1.0
0.8
0.6
0.4
0.2
0.0
Cl2/Asn=1
Cl2/Asn=2
Cl2/Asn=10
Cl2/Asn=20
Chlorination
Chloramination

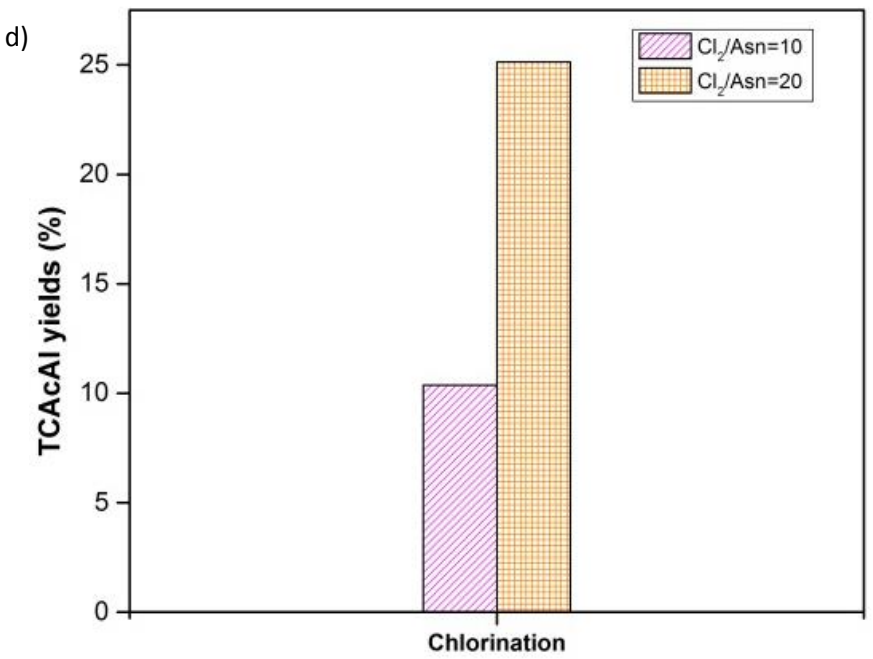

Figure 21. The formation of (a) DCAN, (b) DCAcAm (c) DCAcAl and (d) TCAcAl during the chlorination and chloramination of asparagine as a function of NH_2Cl/asparagine molar ratio, initial asparagine 250 µmol/L, pH 7, 2h, 20 ^oC

As shown in Figure 21 a), DCAN concentration was increased with the increasing chlorine and monochloramine dosages. The DCAN formation at a ratio of 20 by chlorination (3.1% molar yield) was lower than by chloramination (8.8 % molar yield). No DCAN was detected from chloramination when the ratio was 1 and 2. However, DCAcAm formation increased with the increasing ratio (Cl_2/asparagine=1,2,10), then exhibited a decrease when the ratio was 20 both in chlorination and chloramination. This could be related to the oxidation of the amide group in asparagine by the high excess of oxidant (see below). The highest DCAcAm concentration in chlorination and chloramination were 7.8 % and 28.7%, respectively, obtained for a ratio oxidant/asparagine of 10. Moreover, the DCAcAm formation from chloramination was always higher than that from chlorination within all ratios. A similar result was found from previous experiments (see part 3.4.2). Again, this could be explained by the more

important oxidant power of chlorine as compared to monochloramine, thus decomposing the amide group before it can react to form DCAcAm.

As mentioned earlier, aldehydes can be formed during the chlorination and chloramination of α-amino acids. Thus, formation of haloacetaldehydes (HAcAls) was examined in this study.

Contrary to the DCAcAm formation from chloramination, more dichloroacetaldehyde (DCAcAl) and trichloroacetaldehyde (TCAcAl) were detected from chlorination. During chlorination process, DCAcAl and TCAcAl increased with the increasing Cl_2 to asparagine ratio. Especially when the ratio became 10 and 20, the DCAcAl formation were 0.68% and 0.83%, respectively. For TCAcAl, the formation was even higher, with 10.4% and 25.1% molar yield at ratio of 10 and 20, respectively. However, for the chloramination process, the formation of DCAcAl was always lower than 0.07% molar yield, while for TCAcAl, it was always lower than 0.05%. No DCAcAl was detected from chloramination when the ratio was 1.

Higher formation of HAcAls (DCAcAl and TCAcAl) might explain the lower formation of DCAcAm observed by chlorination of asparagine as compared to chloramination. As mentioned earlier (see part 3.4.2) amide group in asparagine, which is the main precursor of DCAcAm formation, might be easily degraded by chlorine.

However, HAcAls have been demonstrated to be the HAcAms precursors through the aldehyde pathway (Kimura et al. 2013). Here, the lack of relationship between HAcAls and HAcAms is due to the fact that the formation of HAcAms from asparagine does not occur via the aldehyde pathway but through halogenation in α of the amide group.

Figure 22 shows the $^{14}N/^{15}N$-DCAN and $^{14}N/^{15}N$-DCAcAm yields from chloramination. The formation of ^{14}N-DCAcAm was increased and then decreased with the increasing Cl_2/ asparagine molar ratio, which corresponded to the total HAcAms formation shown in Figure 21 (b). However, the ^{15}N-DCAcAm formation increased with the increasing Cl_2/ asparagine molar ratio. While DCAcAm was detected at all Cl_2/ asparagine molar ratios, no DCAN was detected at lower ratios (1 and 2). However, a large amount of ^{15}N-DCAN (3.5%) was formed at the Cl_2/ asparagine molar ratio of 20. The formation of DCAcAl from the chloramination of asparagine in the same conditions (Figure 21 (c)), could indicate that ^{15}N-DCAN was produced through the aldehyde pathway.

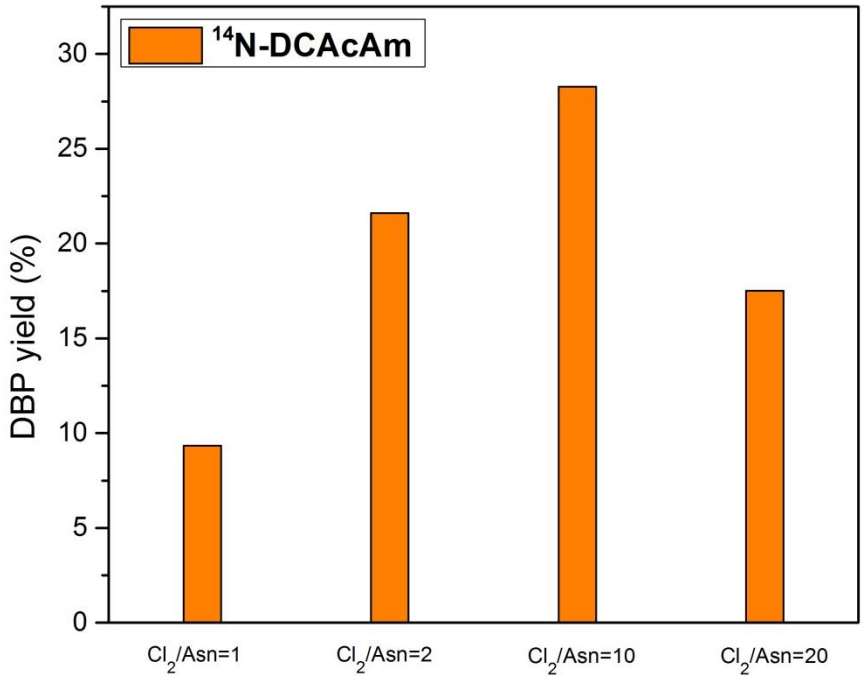

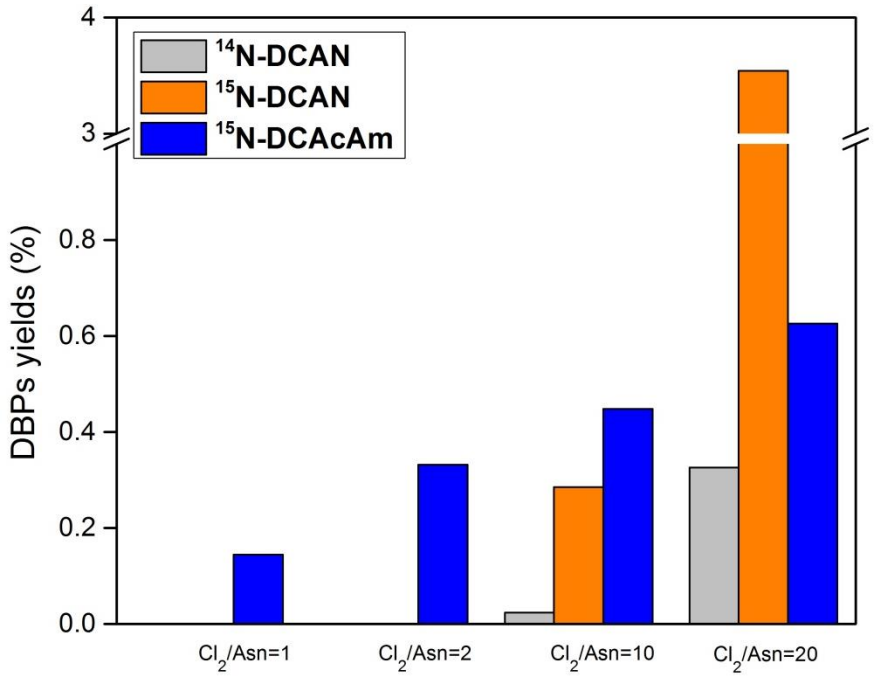

Figure 22. Formation of ^{14}N-DBPs and ^{15}N-DBPs during the chloramination of asparagine as a function of NH_2Cl/asparagine molar ratio, initial asparagine 250 µmol/L, pH 7, 2h, 20 ^{o}C

3.4.4.2 Influence of pH and reaction time

The influence of pH and reaction time on DCAN and DCAcAm formation during chloramination of asparagine was studied. The initial asparagine concentration was 50 µmol/L. The initial monochloramine concentration was 50 mg/L as Cl_2.

Figure 23, shows the DCAcAm and DCAN formation as a function of pH and reaction time. Highest formation of DCAcAm was found at pH 7, followed by pH 5.5, pH 8.8 and pH 11, indicating that DCAcAm formation from asparagine is favored at neutral pH. At pH 8.8 and 11, DCAcAm concentration increased in the first 8h and then decreased. This might be related to the base catalyzed hydrolysis of amide group during long time exposure.

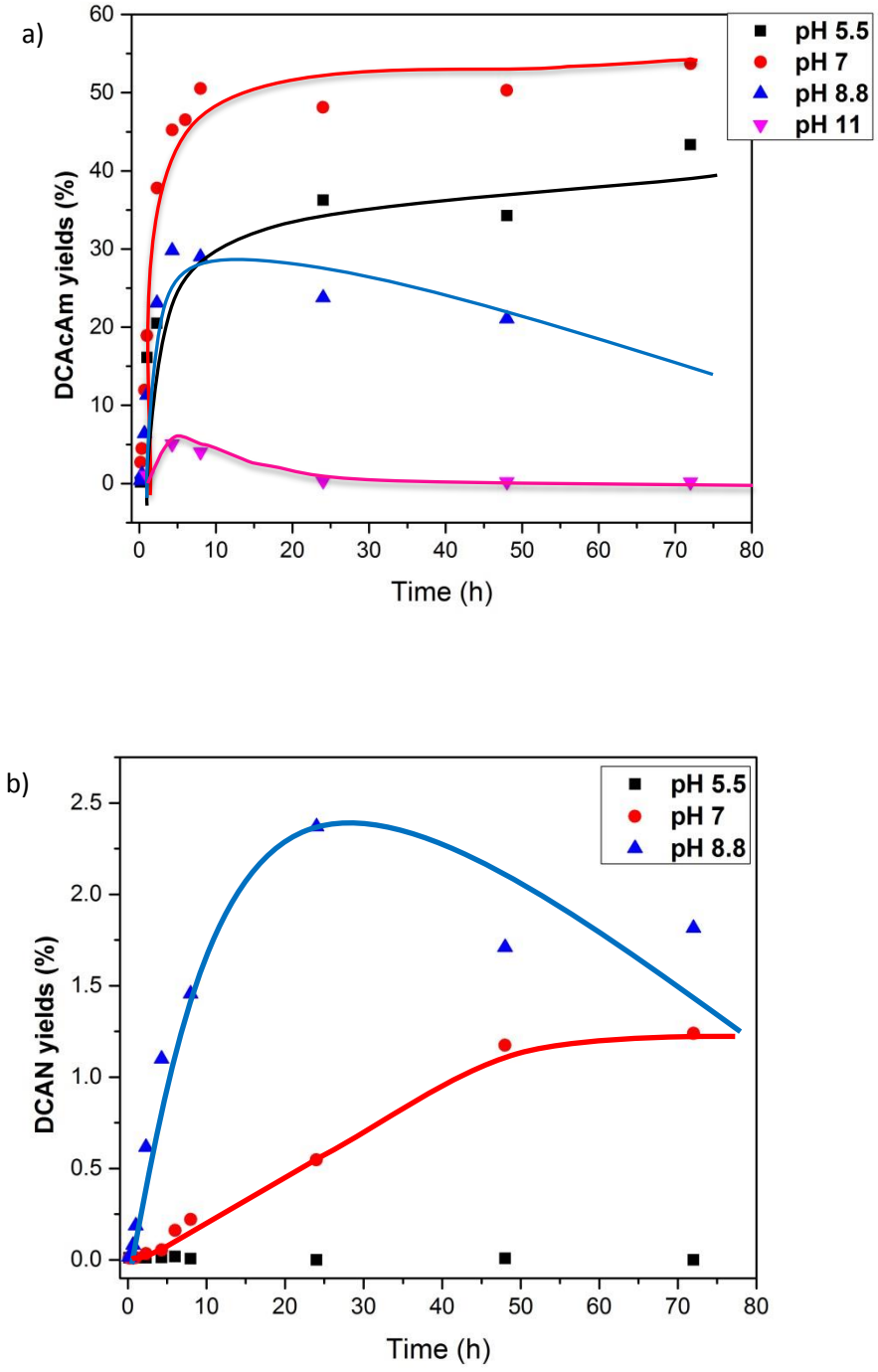

Figure 23. Formation of (a) DCAcAm and (b) DCAN as a function of pH and time during the chloramination of asparagine, initial asparagine 50 µmol/L, initial monochloramine 50 mg/L as Cl_2, 20 ^oC

The highest formation of DCAN was detected at pH 8.8. However, its formation was reduced after 24h. Less than 0.01% DCAN was detected at pH 5.5. No DCAN was found at pH 11. Less formation of DCAN at lower pH and very high pH can be explained by the acid and base catalyzed hydrolysis of DCAN (Reckhow et al. 2001).

Generally, DCAcAm formation was faster than DCAN. For example, at pH 7, DCAcAm was formed rapidly, reaching a concentration of 37.8% molar yield in the first 8 h, and then increased slowly (53.7% at 72h). However, DCAN was formed slowly until 48 h, and then became almost stable. As shown in part 3.4.3, after 72h chloramination of asparagine at pH 7, up to 90% of DCAN nitrogen was coming from monochloramine, while about 98.3% DCAcAm originated from organic nitrogen. This result suggests rapid formation of HAcAms from organic nitrogen, followed by a slow incorporation of inorganic nitrogen coming from monochloramine to form HANs, in accordance with previous literature (Huang et al. 2012).

pH and exposure time do not only affect the stability of N-DBPs and asparagine, but they can also influence the distribution and stability of chloramine species. Dichloramine ($NHCl_2$) is the main species when the pH is lower than 5.5 (see 1.literature review). Even lower pH enhances the formation of nitrogen trichloride (NCl_3). Further studies are needed to investigate the influence of different chloramine species on the formation of N-DBPs.

3.5 N-DBPs formation from phenol and resorcinol

As mentioned earlier, high inorganic nitrogen incorporation was found from the chloramination of *Trichodesmium* sp. AOM and *Hymenomonas* sp. sample collected during death phase, which was more enriched in humic like substances (i.e., high aromatic character). Aromatic amino acids (i.e., tryptophan and tyrosine) were also demonstrated to be important precursor of N-DBPs. In order to investigate the reactivity of aromatic compounds with monochloramine, N-DBPs formation tests were conducted with phenol and resorcinol. The same experimental conditions were applied than previously described for amino acids. 250 µmol/L of phenol or resorcinol was chloraminated for 72h, at pH 7. Initial monochloramine concentration was 100 mg/L as Cl_2.

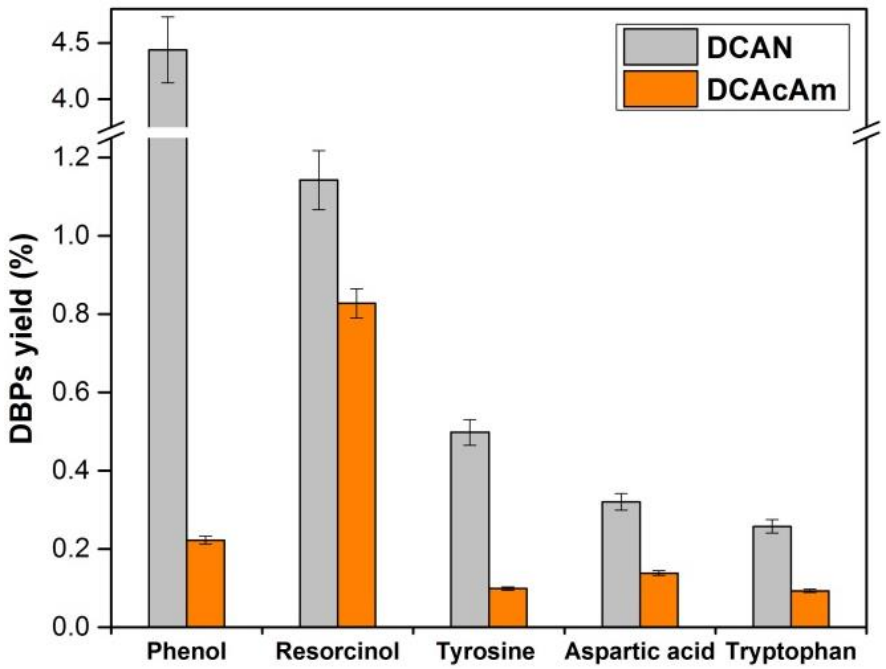

Figure 24. DBPs formation from the chloramination of phenol, resorcinol, tyrosine, aspartic acid and tryptophan, initial concentration of organic compound: 250 µmol/L, Initial monochloramine was 100 mg/L as Cl_2, pH 7, 72 h, 20 ^{o}C

Figure 24 plots DCAN and DCAcAm formation from the chloramination of phenol and resorcinol, compared to the previously studied amino acids (tyrosine, aspartic acid and tryptophan). Phenol and resorcinol formed higher amounts of DCAN and DCAcAm than the amino acids, proving that aromatic compounds can be major precursors of N-DBPs, as compared to previously proposed nitrogenous precursors. Phenol produced the highest amount of DCAN (4.43% molar yield), while the highest proportion of DCAcAm was obtained from resorcinol (0.83%). This can be related to the presence of the second hydroxyl group in meta position, known to activate the aromatic ring for electrophilic substitution by chlorine. N-DBPs formation from phenol and resorcinol confirms the possibility of ring opening during chlorination/chloramination of aromatic amino acids (histidine, tyrosine and tryptophan) (see part 3.4.2)

The high formation potential of DCAN and DCAcAm from phenolic compounds suggests that the presence of organic nitrogen is not necessary to form N-DBPs. Organic compounds without nitrogen (especially aromatic compounds) can react with monochloramine to produce N-DBPs through inorganic nitrogen incorporation. This is of great importance for water treatment facilities using chloramine as the disinfectant, where the removal of high concentrations of aromatic NOM must be optimized to avoid the production of N-DBPs.

4. Conclusions

AOM, bromide and iodide ions in seawater were highly reactive with chlorine and chloramine to enhance the formation of a variety of DBPs. Emerging classes of DBPs (i.e., N-DBPs, brominated and iodinated DBPs) were detected, which are known to be highly toxic. Brominated DBPs (bromoform, DBAA, DBAN and DBAcAm) were the dominant species after 72h chlorination and chloramination.

AOM was found to incorporate important precursors of nitrogenous DBPs (N-DBPs). High formation of N-DBPs was found from *Hymenomonas* sp. samples in exponential growth phase, which was enriched in nitrogenous organic compounds (protein-like). However, high inorganic nitrogen incorporation was observed during the chloramination of algal samples enriched in humic-like compounds (e.g., *Trichodesmium* sp. algal bloom AOM and *Hymenomonas* sp. AOM collected during death phase).

Chloramination reduced the formation of THMs and HAAs as compared to chlorination, however, N-DBPs showed various trends among the samples. In general, chloramination of amino-acids reduced the production of N-DBPs (HANs, HAcAms), while chloramination of *Trichodesmium* sp. algal bloom AOM formed similar or even higher amounts of N-DBPs than chlorination. This indicated the presence of specific precursors of N-DBPs in the *Trichodesmium* sample. More than 50 % of N-DBPs originated from inorganic nitrogen (NH_2Cl) during the chloramination of AOM. This was attributed to the reactivity of humic-like compounds present in AOM. Moreover, chloramines were found to produce N-DBPs from aromatic molecules that don't contain nitrogen atoms (i.e., phenol and resorcinol), indicating that the nature of organic matter (e.g., aromaticity) is

an important parameter influencing N-DBPs formation. Humic substances with aromatic character were found to be highly reactive with monochloramine to produce N-DBPs.

Asparagine, aspartic acid and other amino acids with an aromatic structure were found to be important precursors of HAcAms and DCAN. The amine group was not the main precursor of N-DBPs, but the presence of an activated aromatic ring was a critical parameter influencing the formation of N-DBPs by incorporation of nitrogen from NH_2Cl. The N-DBPs formation potential was impacted by the Cl_2/amino acid molar ratio and pH. Asparagine was a major precursor of HAcAms during chloramination, because of the presence of an amide group in its structure. As opposed to the previous literature, chlorination of asparagine formed less HAcAms than chloramination. A high chlorine dose could oxidize the amide group, further reducing the production of HAcAms.

N-DBPs formation kinetics from asparagine suggested a rapid formation of DCAcAm from organic nitrogen (amide group) and a slower incorporation of inorganic nitrogen coming from monochloramine to form DCAN. The inorganic nitrogen incorporation percentages into HANs and HAcAms were found to be different, suggesting different formation pathways.

REFERENCES

Bichsel, Y. and Von Gunten, U. (1999) Oxidation of iodide and hypoiodous acid in the disinfection of natural waters. Environmental Science and Technology 33(22), 4040-4045.

Bichsel, Y. and Von Gunten, U. (2000) Formation of iodo-trihalomethanes during disinfection and oxidation of iodide-containing waters. Environmental Science and Technology 34(13), 2784-2791.

Bond, T., Huang, J., Templeton, M.R. and Graham, N. (2011) Occurrence and control of nitrogenous disinfection by-products in drinking water - A review. Water Research 45(15), 4341-4354.

Bond, T., Templeton, M.R. and Graham, N. (2012) Precursors of nitrogenous disinfection by-products in drinking water--A critical review and analysis. Journal of Hazardous Materials 235-236, 1-16.

Bousher, A., Brimblecombe, P. and Midgley, D. (1989) Kinetics of reactions in solutions containing monochloramine and bromide. Water Research 23(8), 1049-1058.

Brown, M.R., Garland, C.D., Jeffrey, S.W., Jameson, I.D. and Leroi, J.M. (1993) The gross and amino acid compositions of batch and semi-continuous cultures of Isochrysis sp. (clone T.ISO), Pavlova lutheri and Nannochloropsis oculata. Journal of Applied Phycology 5(3), 285-296.

Carrell Morris, J. (1966) The acid ionization constant of HOCl from 5 to 35°. Journal of Physical Chemistry 70(12), 3798-3805.

Chen, W., Westerhoff, P., Leenheer, J.A. and Booksh, K. (2003) Fluorescence Excitation-Emission Matrix Regional Integration to Quantify Spectra for Dissolved Organic Matter. Environmental Science and Technology 37(24), 5701-5710.

Choi, J. and Valentine, R.L. (2002) Formation of N-nitrosodimethylamine (NDMA) from reaction of monochloramine: A new disinfection by-product. Water Research 36(4), 817-824.

Chu, W., Gao, N., Krasner, S.W., Templeton, M.R. and Yin, D. (2012) Formation of halogenated C-, N-DBPs from chlor(am)ination and UV irradiation of tyrosine in drinking water. Environmental Pollution 161, 8-14.

Chu, W., Gao, N., Yin, D. and Krasner, S.W. (2013) Formation and speciation of nine haloacetamides, an emerging class of nitrogenous DBPs, during chlorination or chloramination. Journal of Hazardous Materials 260, 806-812.

Chu, W.h., Gao, N.y. and Deng, Y. (2010a) Formation of haloacetamides during chlorination of dissolved organic nitrogen aspartic acid. Journal of Hazardous Materials 173(1-3), 82-86.

Chu, W.H., Gao, N.Y., Deng, Y. and Krasner, S.W. (2010b) Precursors of dichloroacetamide, an emerging nitrogenous DBP formed during chlorination or chloramination. Environmental Science and Technology 44(10), 3908-3912.

Chuang, Y.H., Lin, A.Y.C., Wang, X.H. and Tung, H.H. (2013) The contribution of dissolved organic nitrogen and chloramines to nitrogenous disinfection byproduct formation from natural organic matter. Water Research 47(3), 1308-1316.

Connell, G.F. (1996) The Chlorination/Chloramination Handbook, American Water Works Association, Denver, CO.

Connick, R.E. and Chia, Y.T. (1959) The hydrolysis of chlorine and its variation with temperature. Journal of the American Chemical Society 81(6), 1280-1284.

Cowman, G.A. and Singer, P.C. (1996) Effect of bromide ion on haloacetic acid speciation resulting from chlorination and chloramination of aquatic humic substances. Environmental Science and Technology 30(1), 16-24.

Desiderio, D.M. and Nibbering, N.M.M. (2010) White's Handbook of Chlorination and Alternative Disinfectants: Fifth Edition.

Dotson, A. and Westerhoff, P. (2009) Occurrence and removal of amino acids during drinking water treatment. Journal / American Water Works Association 101(9), 101-115+118.

Fang, J., Ma, J., Yang, X. and Shang, C. (2010a) Formation of carbonaceous and nitrogenous disinfection by-products from the chlorination of Microcystis aeruginosa. Water Research 44(6), 1934-1940.

Fang, J., Yang, X., Ma, J., Shang, C. and Zhao, Q. (2010b) Characterization of algal organic matter and formation of DBPs from chlor(am)ination. Water Research 44(20), 5897-5906.

Flury, M. and Papritz, A. (1993) Bromide in the natural environment: Occurrence and toxicity. Journal of Environmental Quality 22(4), 747-758.

Fuge, R. and Johnson, C.C. (1986) The geochemistry of iodine - a review. Environmental Geochemistry and Health 8(2), 31-54.

Glezer, V., Harris, B., Tal, N., Iosefzon, B. and Lev, O. (1999) Hydrolysis of haloacetonitriles: Linear free energy relationship. Kinetics and products. Water Research 33(8), 1938-1948.

Gray Jr, E.T., Margerum, D.W. and Huffman, R.P. (1978) Chloramine equilibria and the kinetics of disproportionation in aqueous solution. ACS Symposium Series (82), 264-275.

Hand, V.C. and Margerum, D.W. (1983) Kinetics and mechanisms of the decomposition of dichloramine in aqueous solution. Inorganic Chemistry 22(10), 1449-1456.

Heller-Grossman, L., Idin, A., Limoni-Relis, B. and Rebhun, M. (1999) Formation of cyanogen bromide and other volatile DBPs in the disinfection of bromide-rich lake water. Environmental Science and Technology 33(6), 932-937.

Henderson, R.K., Baker, A., Parsons, S.A. and Jefferson, B. (2008) Characterisation of algogenic organic matter extracted from cyanobacteria, green algae and diatoms. Water Research 42(13), 3435-3445.

Her, N., Amy, G., Park, H.R. and Song, M. (2004) Characterizing algogenic organic matter (AOM) and evaluating associated NF membrane fouling. Water Research 38(6), 1427-1438.

Hong, H.C., Wong, M.H. and Liang, Y. (2009) Amino acids as precursors of trihalomethane and haloacetic acid formation during chlorination. Archives of Environmental Contamination and Toxicology 56(4), 638-645.

Hua, G. and Reckhow, D.A. (2007) Comparison of disinfection byproduct formation from chlorine and alternative disinfectants. Water Research 41(8), 1667-1678.

Hua, G., Reckhow, D.A. and Kim, J. (2006) Effect of bromide and iodide ions on the formation and speciation of disinfection byproducts during chlorination. Environmental Science and Technology 40(9), 3050-3056.

Huang, H., Wu, Q.Y., Hu, H.Y. and Mitch, W.A. (2012) Dichloroacetonitrile and dichloroacetamide can form independently during chlorination and chloramination of drinking waters, model organic matters, and wastewater effluents. Environmental Science and Technology 46(19), 10624-10631.

Huang, H., Wu, Q.Y., Tang, X., Jiang, R. and Hu, H.Y. (2013) Formation of haloacetonitriles and haloacetamides during chlorination of pure culture bacteria. Chemosphere 92(4), 375-381.

Huang, J., Graham, N., Templeton, M.R., Zhang, Y., Collins, C. and Nieuwenhuijsen, M. (2009) A comparison of the role of two blue-green algae in THM and HAA formation. Water Research 43(12), 3009-3018.

Hureiki, L., Croué, J.P. and Legube, B. (1994) Chlorination studies of free and combined amino acids. Water Research 28(12), 2521-2531.

Kimura, S.Y., Komaki, Y., Plewa, M.J. and Mariñas, B.J. (2013) Chloroacetonitrile and N,2-dichloroacetamide formation from the reaction of chloroacetaldehyde and monochloramine in water. Environmental Science and Technology 47(21), 12382-12390.

Lee, W. and Westerhoff, P. (2009) Formation of organic chloramines during water disinfection - chlorination versus chloramination. Water Research 43(8), 2233-2239.

Li, L., Gao, N., Deng, Y., Yao, J. and Zhang, K. (2012) Characterization of intracellular & extracellular algae organic matters (AOM) of Microcystic aeruginosa and formation of AOM-associated disinfection byproducts and odor & taste compounds. Water Research 46(4), 1233-1240.

Luong, T.V., Peters, C.J. and Perry, R. (1982) Influence of bromide and ammonia upon the formation of trihalomethanes under water-treatment conditions. Environmental Science and Technology 16(8), 473-479.

Morris, J.C. and Isaac, R.A. (1983) Critical review of kinetic and thermodynamic constants for the aqueous chlorine-ammonia system, pp. 49-62.

Muellner, M.G., Wagner, E.D., McCalla, K., Richardson, S.D., Woo, Y.T. and Plewa, M.J. (2007) Haloacetonitriles vs. regulated haloacetic acids: Are nitrogen-containing DBFs more toxic? Environmental Science and Technology 41(2), 645-651.

Myklestad, S.M. (1995) Release of extracellular products by phytoplankton with special emphasis on polysaccharides. Science of The Total Environment 165(1–3), 155-164.

Nagy, J.C., Kumar, K. and Margerum, D.W. (1988) Non-metal redox kinetics: Oxidation of iodide by hypochlorous acid and by nitrogen trichloride measured by the pulsed-accelerated-flow method. Inorganic Chemistry 27(16), 2773-2780.

Nguyen, M.L., Westerhoff, P., Baker, L., Hu, Q., Esparza-Soto, M. and Sommerfeld, M. (2005) Characteristics and reactivity of algae-produced dissolved organic carbon. Journal of Environmental Engineering 131(11), 1574-1582.

Pedersen III, E.J., Urbansky, E.T., Mariñas, B.J. and Margerum, D.W. (1999) Formation of cyanogen chloride from the reaction of monochloramine with formaldehyde. Environmental Science and Technology 33(23), 4239-4249.

Plewa, M.J., Kargalioglu, Y., Vankerk, D., Minear, R.A. and Wagner, E.D. (2002) Mammalian cell cytotoxicity and genotoxicity analysis of drinking water disinfection by-products. Environmental and Molecular Mutagenesis 40(2), 134-142.

Plewa, M.J., Muellner, M.G., Richardson, S.D., Fasano, F., Buettner, K.M., Woo, Y.T., McKague, A.B. and Wagner, E.D. (2008) Occurrence, synthesis, and mammalian cell cytotoxicity and genotoxicity of haloacetamides: An emerging class of nitrogenous drinking water disinfection byproducts. Environmental Science and Technology 42(3), 955-961.

Plewa, M.J., Wagner, E.D., Jazwierska, P., Richardson, S.D., Chen, P.H. and McKague, A.B. (2004) Halonitromethane Drinking Water Disinfection Byproducts: Chemical Characterization and Mammalian Cell Cytotoxicity and Genotoxicity. Environmental Science and Technology 38(1), 62-68.

Plummer, J.D. and Edzwald, J.K. (2002) Effects of chlorine and ozone on algal cell properties and removal of algae by coagulation. Journal of Water Supply: Research and Technology - AQUA 51(6), 307-318.

Reckhow, D.A., MacNeill, A.L., Platt, T.L., MacNeill, A.L. and McClellan, J.N. (2001) Formation and degradation of dichloroacetonitrile in drinking waters. Journal of Water Supply: Research and Technology - AQUA 50(1), 1-13.

Reckhow, D.A. and Singer, P.C. (1986) Mechanisms of organic halide formation during fulvic acid chlorination and implications with respect to preozonation, pp. 1229-1257.

Richardson, S.D., Fasano, F., Ellington, J.J., Crumley, F.G., Buettner, K.M., Evans, J.J., Blount, B.C., Silva, L.K., Waite, T.J., Luther, G.W., McKague, A.B., Miltner, R.J., Wagner, E.D. and Plewa, M.J. (2008) Occurrence and mammalian cell toxicity of iodinated disinfection byproducts in drinking water. Environmental Science and Technology 42(22), 8330-8338.

Richardson, S.D., Plewa, M.J., Wagner, E.D., Schoeny, R. and DeMarini, D.M. (2007) Occurrence, genotoxicity, and carcinogenicity of regulated and emerging disinfection by-products in drinking water: A review and roadmap for research. Mutation Research - Reviews in Mutation Research 636(1-3), 178-242.

Rook, J.J. (1975) Formation of and occurence of haloforms in drinking water.

Rostad, C.E., Leenheer, J.A. and Daniel, S.R. (1997) Organic carbon and nitrogen content associated with colloids and suspended particulates from the Mississippi River and some of its tributaries. Environmental Science and Technology 31(11), 3218-3225.

Shah, A.D. and Mitch, W.A. (2012) Halonitroalkanes, halonitriles, haloamides, and N-nitrosamines: A critical review of nitrogenous disinfection byproduct formation pathways. Environmental Science and Technology 46(1), 119-131.

Symons, J.M., Krasner, S.W., Simms, L.A. and Sclimenti, M. (1993) Measurement of THM and precursor concentrations revisited: the effect of bromide ion. Journal / American Water Works Association 85(1), 51-62.

Trofe, T.W. (1980) Kinetics of monochloramine decomposition in the presence of bromide. Environmental Science and Technology 14(5), 544-549.

Ueno, H., Moto, T., Sayato, Y. and Nakamuro, K. (1996) Disinfection by-products in the chlorination of organic nitrogen compounds: By-products from kynurenine. Chemosphere 33(8), 1425-1433.

USEPA (1999) Alternative Disinfectants and Oxidants Guidance Manual. EPA 815-R-99-014.

Vikesland, P.J., Ozekin, K. and Valentine, R.L. (2001) Monochloramine decay in model and distribution system waters. Water Research 35(7), 1766-1776.

Westerhoff, P., Chao, P. and Mash, H. (2004) Reactivity of natural organic matter with aqueous chlorine and bromine. Water Research 38(6), 1502-1513.

Westerhoff, P. and Mash, H. (2002) Dissolved organic nitrogen in drinking water supplies: A review. Journal of Water Supply: Research and Technology - AQUA 51(8), 415-448.

Xie, P., Ma, J., Fang, J., Guan, Y., Yue, S., Li, X. and Chen, L. (2013) Comparison of permanganate preoxidation and preozonation on algae containing water: Cell integrity, characteristics, and chlorinated disinfection byproduct formation. Environmental Science and Technology 47(24), 14051-14061.

Yang, X., Fan, C., Shang, C. and Zhao, Q. (2010) Nitrogenous disinfection byproducts formation and nitrogen origin exploration during chloramination of nitrogenous organic compounds. Water Research 44(9), 2691-2702.

Yang, X., Shang, C. and Westerhoff, P. (2007) Factors affecting formation of haloacetonitriles, haloketones, chloropicrin and cyanogen halides during chloramination. Water Research 41(6), 1193-1200.

Yang, X., Shen, Q., Guo, W., Peng, J. and Liang, Y. (2012) Precursors and nitrogen origins of trichloronitromethane and dichloroacetonitrile during chlorination/chloramination. Chemosphere 88(1), 25-32.

Zimmerman, G. and Strong, F.C. (1957) Equilibria and spectra of aqueous chlorine solutions. Journal of the American Chemical Society 79(9), 2063-2066.

APPENDICES

Table 10. HAcAms and HAAs formation from the chlorination of 20 amino acids, initial amino acid: 5 µmol/L, initial chlorine: 5 mg/L as Cl_2, pH 7, 20 ^oC, 72 h

	DCAcAm µg/L	DCAcAm molar yield (%)	TCAcAm µg/L	TCAcAm molar yield (%)	DCAA µg/L	DCAA molar yield (%)	TCAA µg/L	TCAA molar yield (%)
Glycine	0.024	0.004	0.087	0.011	0.777	0.121	0.564	0.069
Alanine	0.010	0.001	0.153	0.019	0.000	0.000	0.492	0.060
Serine	0.005	0.001	0.088	0.011	0.873	0.135	0.662	0.081
Threonine	0.006	0.001	0.040	0.005	0.817	0.127	0.530	0.065
Cysteine	0.015	0.002	0.104	0.013	0.617	0.096	0.392	0.048
Valine	0.000	0.000	0.066	0.008	0.696	0.108	0.550	0.067
Leucine	0.015	0.002	0.032	0.004	0.737	0.114	0.537	0.066
Isoleucine	0.000	0.000	0.004	0.001	0.771	0.120	0.652	0.080
Methionine	0.007	0.001	0.110	0.013	1.072	0.166	0.907	0.111
Proline	0.023	0.004	0.057	0.007	0.761	0.118	0.607	0.074
Phenylalanine	0.022	0.003	0.079	0.010	0.490	0.076	0.409	0.050
Tyrosine	0.000	0.000	10.723	1.313	17.263	2.678	83.649	10.239
Tryptophan	0.000	0.000	9.028	1.105	32.068	4.974	107.779	13.193
Aspartic acid	31.896	4.992	0.273	0.033	91.660	14.217	0.880	0.108
Glutamic acid	0.022	0.003	0.086	0.011	0.646	0.100	0.579	0.071
Asparagine	28.299	4.429	2.314	0.283	59.736	9.266	2.627	0.322
Glutamine	0.014	0.002	0.133	0.016	0.838	0.130	0.574	0.070
Histidine	0.000	0.000	1.924	0.236	20.839	3.232	12.321	1.508
Lysine	0.046	0.007	0.069	0.008	0.565	0.088	0.550	0.067
Arginine	0.035	0.006	0.098	0.012	1.219	0.189	1.020	0.125